Natural Resources Canada
Ressources naturelles Canada

GEOLOGICAL SURVEY OF CANADA
OPEN FILE 7904

Geotechnical data from a large landslide site at Quyon, Quebec

B. Wang, G.R. Brooks, J.A.M. Hunter

2015

Canada

GEOLOGICAL SURVEY OF CANADA
OPEN FILE 7904

Geotechnical data from a large landslide site at Quyon, Quebec

B. Wang, G.R. Brooks, J.A.M. Hunter

2015

doi:10.4095/297049

Recommended citation

Wang, B., Brooks, G.R., and Hunter J.A.M., 2015. Geotechnical data from a large landslide site at Quyon, Quebec; Geological Survey of Canada, Open File 7904, 54 p. doi:10.4095/297049

Geotechnical data from a large landslide site at Quyon, Quebec

Baolin Wang, Gregory R. Brooks, James A.M. Hunter

ABSTRACT

A geotechnical study was initiated in 2014 to investigate the triggering mechanism of an enormous prehistorical landslide near Quyon, Quebec. The study consisted of surveys of the thickness of the glaciolacustrine deposits with a hand held seismograph, cone penetrometer testing (CPT), seismic cone penetrometer testing (SCPT), field vane shear testing (VST), soil sampling, and laboratory testing. Preliminary results were presented in a separate paper. This Open File provides more detailed information and updated data. In summary, the measured thickness of the Champlain Sea deposits in the region ranges from 0 m (at bedrock outcrops) to 68 m. The underlying bedrock surface forms a buried valley underlying the modern Quyon River. The glaciomarine sediments consist of clay, silty clay or clayey silt. The materials from the southern area are finer than that of the northern area. The materials in the southern area exhibit a high to extremely high plasticity with Plasticity Index ranging from 38.6% to 68.6%. The materials from the northern area have low to high plasticity with the Plasticity Index ranging from 13.9% to 33.0%. The clay/silt samples from 30 m depth and above have moisture content higher than the liquid limit in both the northern and southern areas. The CPT bearing factor N_{kt} was calibrated to be 11.5. The pore pressure bearing factor $N_{\Delta u}$ varies with pore water pressure parameter B_q. The soil undrained shear strength (S_u) ranges from 22 kPa to 250 kPa. The S_u profiles determined from N_{kt} and $N_{\Delta u}$ are identical. A clay unit of continuous S_u profile was identified at three CPT locations in the undisturbed areas outside the landslide scar. Absence of the low strength material and discontinuity of the S_u profiles were observed at upper elevations in the drill holes inside the landslide scar, which suggest that the upper clay unit either flowed away or was dislocated.

1. INTRODUCTION

An enormous landslide was identified near Quyon, Quebec by Brooks (2013). The landslide (referred to as Quyon landslide in this Open File) covers an area of approximately 14 km long and 4 km wide within Champlain Sea glaciomarine deposits along the Quyon River (Fig. 1). It is associated with prehistoric failures of the sensitive Champlain Sea glaciomarine deposits along the lower Quyon River valley. Brooks (2013) interpreted that the landslide zone is primarily the product of a massive failure that occurred between 980 and 1060 calibrated years before present (cal. YBP). He hypothesized that the failure was triggered by a prehistoric earthquake, based on the common radiocarbon ages of the Quyon landslide and nine other landslides in the Quyon-Ottawa area. The magnitude of the triggering earthquake was estimated to be at least M_w 6.1 based on the empirical landslide area – earthquake magnitude relationship of Keefer (1984) and Rodriguez et al. (1999). In order to improve the estimation of this magnitude, a geotechnical investigation was initiated at the Geological Survey of Canada (GSC), Natural Resources Canada, in 2014. The first phase of the study consisted of surveys of the thickness of the glaciolacustrine deposits across the Quyon landslide area, cone penetrometer testing (CPT), seismic cone penetrometer testing (SCPT), field vane shear testing (VST), soil sampling, and laboratory testing. Preliminary results were presented by Wang et al. (2015). This Open File provides detailed geotechnical data and updates.

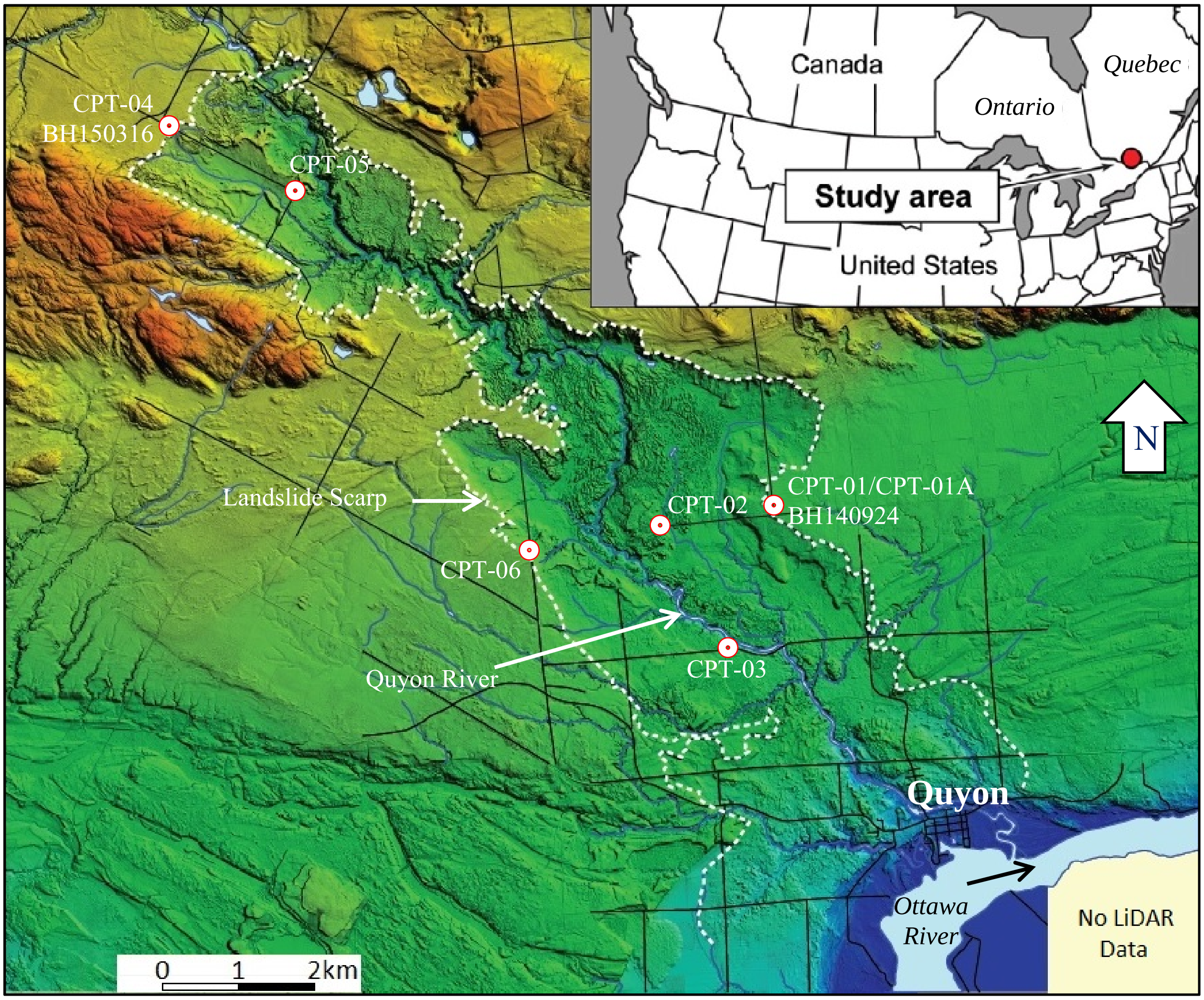

Fig. 1. Location map of study area based on LiDAR image (LiDAR image © Government of Quebec)

2. STUDY AREA

Quyon River is a tributary of the Ottawa River (Fig. 1). It is located in southwestern Quebec, about 44 km WNW of Ottawa, Ontario. The landslide area developed within Champlain Sea sediments along the Quyon River Valley (St.-Onge, 2009). The sediments were deposited between 13.9 and 11.5 ka cal BP (Dyke and Prest, 1987). Locally, the deposits are composed of 3 to 4 m of sand capping glaciomarine clay and silty clay of varying thickness that overlies bedrock (Gadd, 1986). The Champlain Sea deposits became incised by the postglacial stream network in the early Holocene as the Champlain Sea receded because of regional postglacial uplift (Gadd, 1987).

Little geotechnical information has been published on the Champlain Sea deposits within the Quyon Valley. Gadd (1986), however, reports "very sensitive" clay between 13.7 and 17.7 m depth from a geological borehole (#76-20) located on the Champlain Sea plain, 2~3 km north of the village of Quyon. In a second borehole (#76-18) located nearby, but within the landslide scar, "distorted" and/or "tilted" deposits were recovered to 14.4 m depth. The landslide area is primarily agricultural, consisting of cultivated fields, pasture, and woodlands. The village of Quyon is located in the southern part of the area along the Ottawa River (Fig. 1).

3. METHODS

3.1 Survey of Champlain Sea Sediment Thickness

Microtremor surveys were carried out to map the thickness of the Champlain Sea Sediments within the Quyon landslide zone. A portable 3-component Tromino™ seismograph designed for horizontal to vertical spectral ratio (HVSR) measurements was used for the survey. In areas where the thickness of soft soil (with low shear wave velocities) exceeds about 10 m and overlies competent bedrock or firm soil (with high shear wave velocities), ground resonance will occur at the site's fundamental period, T_0, as a function of the shear wave velocity and the thickness of the soil unit (Kramer, 1996):

$$T_0 = 4\,H / V_s \qquad (1)$$

where H = soil thickness;
V_s = average shear wave velocity of the soil unit.

In the general Ottawa area, the predominant seismic impedance boundary is the base of the soft Champlain Sea sediments overlying glacial sediments (ice-contact or glaciofluvial sediments) or, Paleozoic or Precambrian bedrock (if glacial sediments are absent). This stratigraphy typically exhibits a strong impedance contrast and yields a well-defined sharp peak period (resonant period). Dobry et al. (1976) has shown that a shear wave velocity gradient within young (Holocene age) unconsolidated sediments can alter the observed fundamental period and the estimated "effective depth" to the resonator. Hunter et al. (2010), using borehole and seismic reflection data, developed an empirical relationship between the thickness of the soft sediment and the resonant period for the typical Champlain Sea deposits in the general Ottawa area:

$$H = 56.7\,T_0^{1.48} \pm 6.1 \text{ (m)} \qquad (2)$$

This correlation was used to interpret the soft sediment thickness from the HVSR measurements in the Quyon landslide area.

3.2 Cone Penetrometer Tests

Seven Cone Penetrometer Tests (CPT) were conducted at six locations on August 19, 2014 and January 14 to 15, 2015 by ConeTec Investigations Ltd. and supervised by GSC personnel. The test locations are shown in Fig. 1. The location coordinates and tests conducted are listed in Table 1. All CPT tests were done on road shoulders.

A 25 ton tire truck mounted CPT rig was used for the cone penetration tests. The tests were carried out using an integrated electronic cone penetration testing and data acquisition system. The cone and rods were pushed into the ground using a hydraulic ramset located inside the rig, at a steady rate of 2 cm/s. The CPT soundings were completed in accordance with ASTM D5778.

Table 1. Drill hole locations and tests conducted

Site #	Location	Depth (m)	CPT	SCPT	VST	Shelby Samples	Note
CPT-01	N45º33'24.6 W76º15'42.3	32.6	✓		✓	✓	BH140924 (15 m east of CPT-01) CPT-01A (10 m south of CPT-01) Undisturbed, outside landslide scar.
CPT-02	N45º33'17.5 W76º16'46.2	43.9	✓				Disturbed, inside landslide scar.
CPT-03	N45º32'24.6 W76º16'09.2	25.7	✓				Disturbed, inside landslide scar.
CPT-04	N45º36'07.5 W76º21'47.9	55.2	✓	✓	✓	✓	BH150316 (10 m south of CPT-04) Undisturbed, outside landslide scar.
CPT-05	N45º35'39.8 W76º20'32.0	39.4	✓				Disturbed, inside landslide scar.
CPT-06	N45º33'05.5 W76º18'09.2	23.0	✓				Undisturbed, outside landslide scar.

The cone used at CPT-01 through CPT-03 had a maximum tip capacity of 100 MPa, a tip area (A_c) of 10 cm^2, a friction sleeve area (A_s) of 150 cm^2, and a pore pressure transducer capacity of 3.4 MPa (500 psi). The cone used at CPT-04 through CPT-06 had a maximum tip capacity of 150 MPa, a tip area (A_c) of 15 cm^2, a friction sleeve area (A_s) of 225 cm^2, and a pore pressure transducer capacity of 3.4 MPa (500 psi). The piezocones have a platinum resistive temperature device for monitoring the temperature of the sensors. The 10 cm^2 piezocone uses a friction reducer consisting of a rod adapter extension behind the main cone body with an enlarged cross-sectional area located at a distance of 585 mm above the cone tip. The 15 cm^2 penetrometer does not require a friction reducer as it has a diameter larger than the deployment rods.

A 6 mm thick pore pressure filter was used directly behind the cone tip. The filter, which is composed of porous plastic, enables the cone penetrometer to measure dynamic pore pressures during penetration, and record pore pressure dissipations at selected depths. The function of the filter allows rapid movements of the extremely small volumes of water needed to activate the pressure transducer while preventing soil ingress or blockage. The pore pressure filter was saturated with silicone fluid under vacuum pressure prior to testing and the pore pressure cavity within the cone was filled with silicone fluid to maintain a compliant pore pressure measuring system. The data acquisition system automatically records and displays the pore pressure dissipation traces in real time (at five second intervals) during pauses in penetration.

The CPT cone has an equal end area friction sleeve; hence no corrections are required for friction sleeve data. The cone has an unequal area effect on the tip resistance due to the tip and load cell geometry. The cone net area ratio (*a*) for tip resistance correction is 0.80.

The cone system used during the tests recorded the tip resistance and sleeve friction in kPa and the pore pressure in meters. The data acquisition frequency was every 5 cm.

The interpretation of the CPT data is based on the corrected tip resistance (q_t), sleeve friction (f_s) and pore water pressure (u_2). The interpretation of Soil Behaviour Type (SBT) is based on the correlations developed by Robertson (1990) and Robertson (2009).

The recorded tip resistance (q_c) and the recorded dynamic pore pressure behind the tip (u_2) were used for calculating q_t as follows:

$$q_t = q_c + (1 - a)\, u_2 \qquad (3)$$

where: q_t is the corrected tip resistance
q_c is the recorded tip resistance
u_2 is the recorded dynamic pore pressure behind the tip (at shoulder of the cone)
a is the Net Area Ratio for the piezocone (0.80 for the probes used)

The sleeve friction (f_s) is the frictional force on the sleeve divided by its surface area. As the piezocones used in these tests have equal end area friction sleeves, pore pressure corrections to the sleeve data are not required.

The friction ratio (R_f) is a calculated parameter. It is defined as the ratio of sleeve friction to the tip resistance expressed as a percentage. The friction ratio gives an indication of the grain size characteristics of the material. Generally, saturated cohesive soils have low tip resistance, high friction ratios and generate large excess pore water pressures.

The dynamic pore pressure (u_2) is a measure of the pore pressures generated during cone penetration. To record equilibrium pore pressure, the penetration was stopped to allow the dynamic pore pressures to dissipate. The variation of the pore pressure with time was measured and recorded. All pore pressure data was recorded immediately behind the cone tip (shoulder of the cone).

Seismic cone penetration test (SCPT) was conducted at CPT-04 to measure the shear wave velocity along the drill hole. The cone penetrometer was equipped with a horizontally active geophone (28 hertz) that was rigidly mounted in the body of the cone penetrometer, 0.2 m behind the cone tip. Shear waves were generated by using an impact hammer horizontally striking a steel beam that was held in place on ground surface by a normal load. The active axis of the geophone was aligned parallel to the beam (or source) and the horizontal offset between the cone and the source was 0.6 m. The seismic wave traces were recorded using an up-hole integrated digital oscilloscope, part of the data acquisition system. Prior to recording seismic waves at each test depth, cone penetration is stopped and the rods are decoupled from the rig to avoid transmission of rig energy down the rods. Multiple wave traces were recorded for quality control purposes. After reviewing wave traces for consistency, the cone was pushed to the next test depth at 1 m intervals.

3.3 Soil Sampling and Vane Shear Testing

Soil sampling and field vane shear tests (VST) were carried out at BH140924 on Sept. 24, 2014. Borehole BH140924 is located at about 15 m to the east of CPT-01 and CPT-01A. It is in an undisturbed zone on the crest of the landslide scarp. The drilling and testing were conducted with a tire truck mounted drill rig by OGS Inc. A hollow stem auger of ID 10.8 cm (4¼ inch) was used for the drilling. Shelby tubes with a standard stationary piston sampler were used for undisturbed soil sampling. The Shelby tubes are ID 7.0 cm (2¾ in), OD 7.3 cm (2⅞ in) and length 67.6 cm (26⅝ in). The vane shear tests were carried out in accordance with ASTM D2573 and Shelby sampling with ASTM D1587.

The Shelby sampling and VST were planned for each 4.6 m (15 ft) interval at BH140924. A full Shelby core was retrieved from 4.6 m (15 ft) depth and another from 9.2 m (30 ft) depth. Only a half core was retrieved from the 13.7 m (45 ft) depth. The half core slipped from the top to the bottom of the tube when it was brought up to the surface. Attempts were made to collect samples at 18.3 m (60 ft), 22.9 m (75 ft) and 27.4 m (90 ft) depth. However, the cores were lost halfway in the drill hole during retrieval. The Shelby samples were sealed with wax and transported in accordance with ASTM D4220 to the GSC Sedimentology Laboratory for geotechnical index property testing.

Field vane shear tests were carried out at 35 cm and 65 cm below the bottom of the Shelby hole after the soil sample was retrieved. The geometry of the vane used at BH140924 is shown in Fig. 2. The tests were carried out with torques applied by hand at the top of the rods. Following each peak undrained shear strength test, a remolded undrained shear strength test was conducted after ten vane rotations.

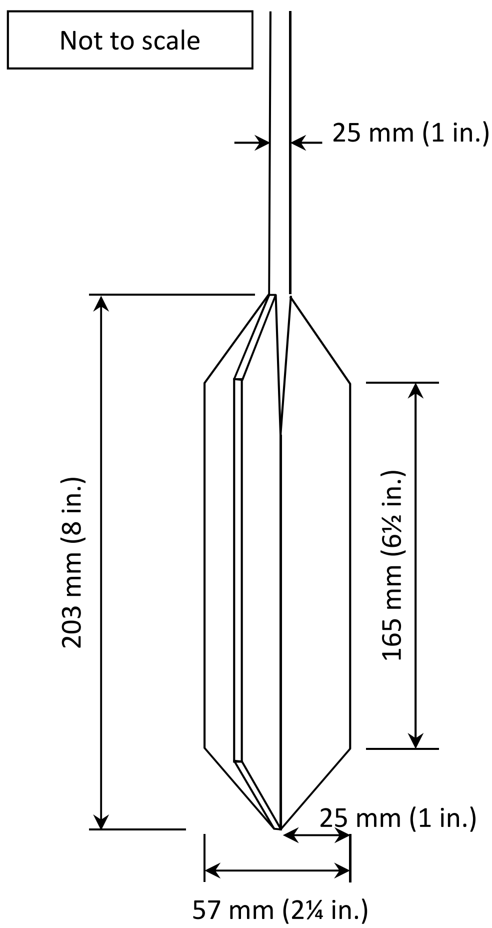

Fig. 2 Geometry of field vane used for soil undrained shear strength test at BH140924

Field vane shear tests were conducted at another site BH150316 on March 16 to 19, 2015. This borehole is located at 10 m south of CPT-04 at an undisturbed zone on the crest of the northern scarp of the landslide. CCC Drilling was contracted for the drilling and testing at BH150316. A track mounted drill rig was used at this site. The drilling was conducted with a hollow stem auger of ID 10.8 cm (4¼ inch). Shelby tubes with a standard stationary piston sampler were used for undisturbed soil sampling. The Shelby tubes are ID 7.0 cm (2¾ in), OD 7.3 cm (2⅞ in) and length 67.6 cm (26⅝ in). Vane shear tests were carried out in accordance with ASTM D2573 and the Shelby sampling with ASTM D1587.

The first planned Shelby sampling depth at BH150316 was 6.1 m (20 ft). However, fine sand was encountered as observed from the drill bit when retrieved from 6.1, 7.6, and 9.1 m (20, 25, and 30 ft) depths. The auger hole was further advanced from 9.1 m (30 ft) to 12.2 m (40 ft) where clay was encountered. The soil sampling and vane shear testing at BH150316 were conducted at: 12.2 m (40 ft), 16.8 m (55 ft), 24.4 m (80 ft), 32.0 m (105 ft), 39.6 m (130 ft), and 47.2 m (155 ft) depths with one Shelby sample followed by two vane shear tests at each interval. A full Shelby core was retrieved from each of the above depths. The Shelby samples were sealed with wax and transported in accordance with ASTM D4220 to the GSC Sedimentology Laboratory for geotechnical index property testing.

The vane shear tests were conducted at the bottom of the Shelby hole immediately after the soil sampling. Two different sized vanes were used at this site. The geometries of the vanes are shown in Fig. 3. The tests were carried out with the larger sized (N-Type) vane in the upper elevations until 25 m depth. It was switched to the smaller (V-type) vane below 25 m where the torque exceeded the limit of the instrument with the larger vane. The tests were carried out with torques applied by hand at the top of the rods. Following each peak undrained shear strength test, the remolded undrained shear strength was measured after ten vane rotations.

The soil undrained shear strength was calculated using the following equation (ASTM D2573-08):

$$S_u = 12\ T_{max} / \{\pi\ D^2\ [2\ D / \cos(\alpha) + 6\ H]\} \qquad (4)$$

where T_{max} = maximum torque;
D = vane diameter;
H = height of vane;
α = angle of taper at top and bottom of vane.

Most vane shear tests were carried out in relatively clean holes where rod frictions were negligible. Where noticeable rod frictions were expected such as when considerable loose materials in the drill hole were suspected, blank rod friction tests were conducted with no vane attached and the VST results were corrected accordingly.

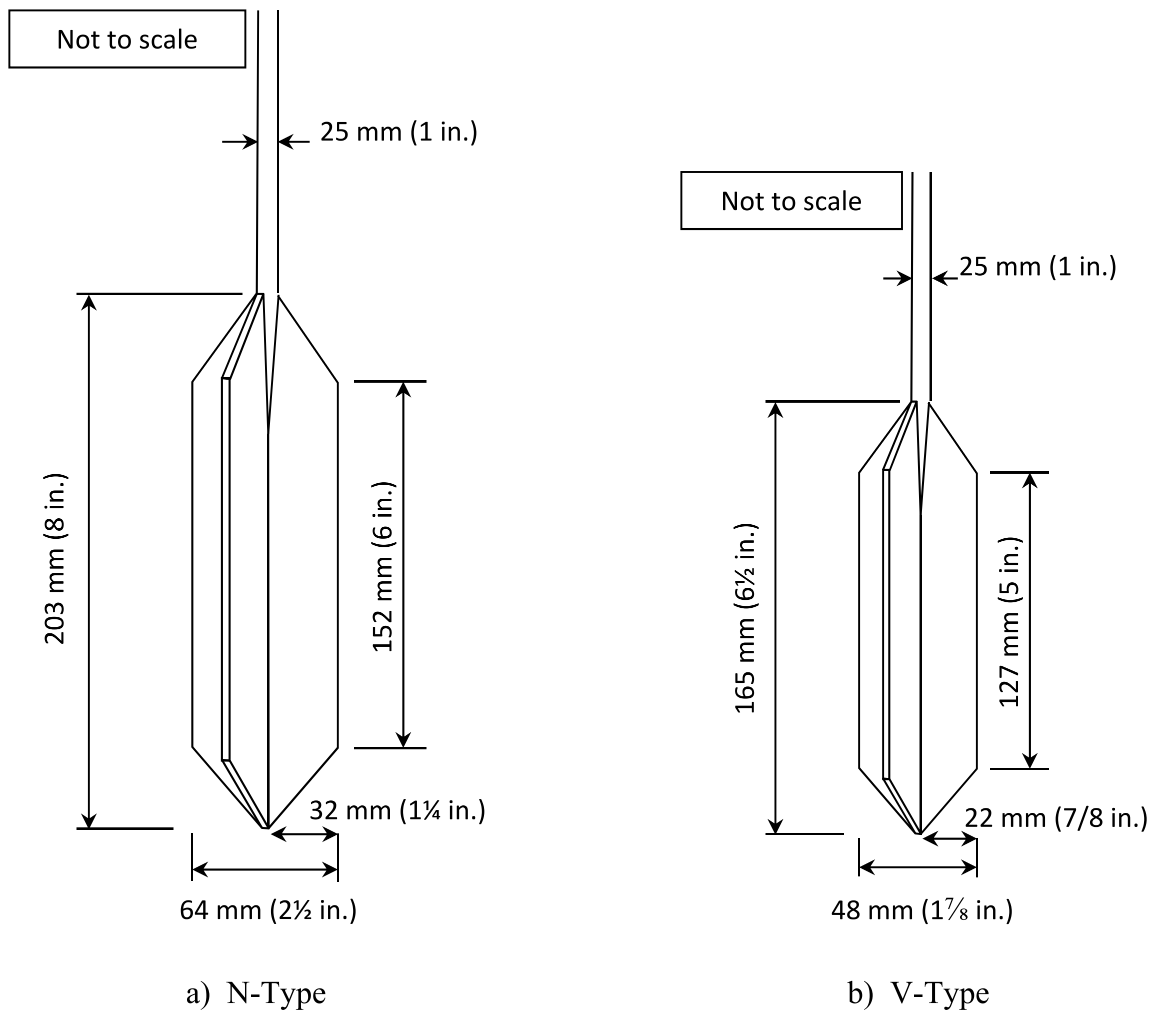

Fig. 3 Geometries of field vanes used for soil undrained shear strength test at BH150316

3.4 Laboratory Tests

The Shelby cores were stored in a refrigerator until extruded for testing. The extruded cores were cut into segments of about 4 cm to 5 cm long. Each sample was then put in a tin container of 8 cm in diameter and 5 cm high. The containers were sealed with electrical tape and refrigerated until testing.

A Pocket Penetrometer CL-7000 manufactured by Soiltest Inc. was used to test the unconfined undrained shear strength of the soil samples. The tests were carried out on the core ends during cutting of the Shelby samples, i.e., on the freshly exposed core face after a core segment was taken. Five readings were taken on each core face and the average value was used as the shear strength of the core.

Soil moisture contents, Atterberg limits, unit weight, specific gravity and gradations were determined in accordance with the respective ASTM standards by the GSC's Sedimentology Laboratory.

4. RESULTS

4.1 Champlain Sea Sediment Thickness

The HVSR measurement of Champlain Sea deposit thickness was carried out at 180 locations inside and outside the Quyon landslide scar. The survey results indicate that the thickness of the Champlain Sea sediments ranges from zero (at rock outcrops) to about 68 m. The LiDAR DEM surface elevation (Fig. 1) and the depth of seismic impedance were used to delineate the base of the sediments. Fig. 4 shows a contour plot of the interpreted base of the Champlain Sea sediments. The outline of the Quyon Landslide is superimposed on the contour map.

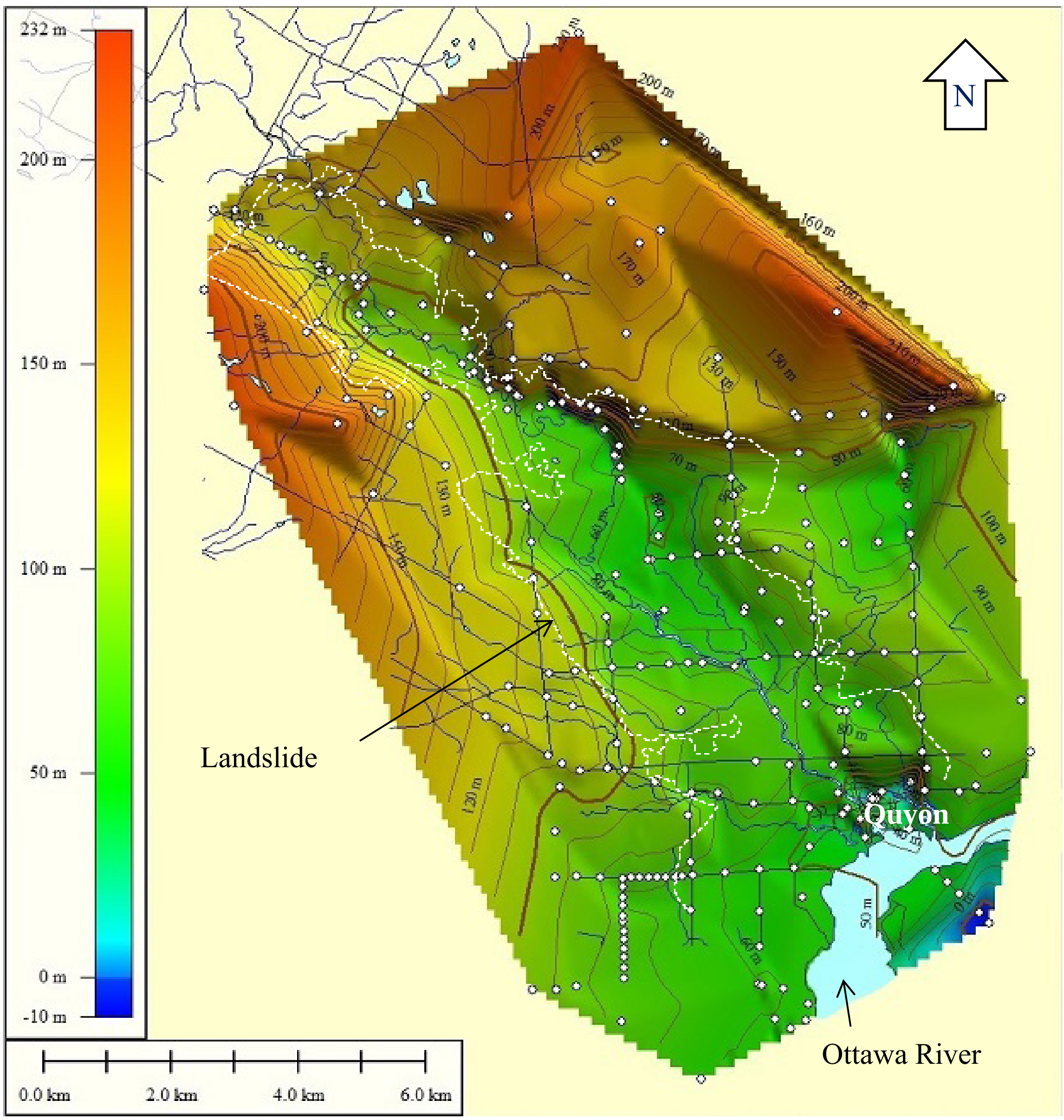

Fig. 4. Seismic impedance profiles indicating the base of the Champlain Sea sediments interpreted from HVSR measurements (Colour shading and contour values indicate impedance elevation asl.). The locations of HVSR measurements are marked with white dots.

The contour plot in Fig. 4 indicates a bedrock valley underlying the Quyon River. The scar of the Quyon landslide was approximately confined by the shape of the bedrock valley. These data were used as guidance for the next stage geotechnical site investigations.

4.2 Borehole Logs and Laboratory Test Results

Borehole logs for the auger holes BH140924 and BH150316 are provided in Appendix A. The laboratory test results of the moisture content, Atterberg limit, unit weight, specific gravity, and the pocket penetrometer shear strength results are included in the borehole logs. Table 2 lists the minimum and maximum values of the geotechnical index properties from the borehole samples. Figs. 5 and 6 are gradation charts of the samples. The soil plasticity charts are shown in Figs. 7 and 8.

Table 2. Range of Geotechnical Index Properties of Soil Samples Collected

Borehole #	Description	W_c (%)	PL (%)	LL (%)	I_p (%)	γ (kN/m^3)	G_s
BH140924	Minimum	67.3	22.5	61.1	38.6	14.4	2.74
	Maximum	108.7	33.4	102.0	68.6	15.8	2.77
BH150316	Minimum	37.6	18.0	31.9	13.9	17.0	2.78
	Maximum	47.3	22.4	54.5	33.0	18.0	2.79

Notes: W_c = water content; PL = plastic limit; LL = liquid limit; I_p = plasticity index; γ = unit weight; G_s = specific gravity

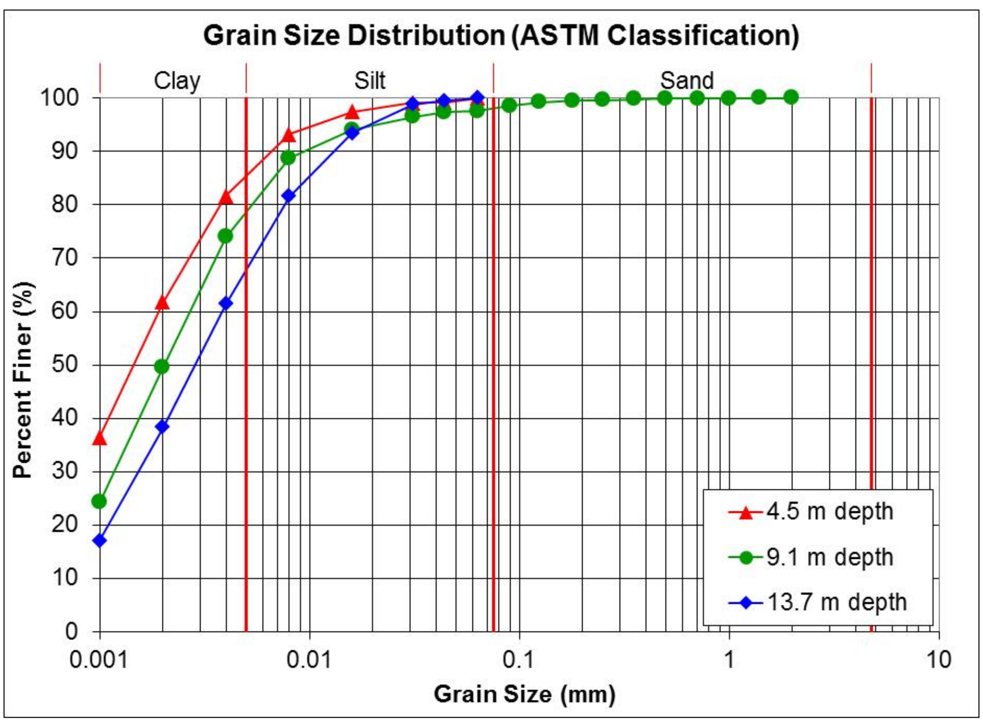

Fig. 5. Gradation chart of soil samples from BH140924

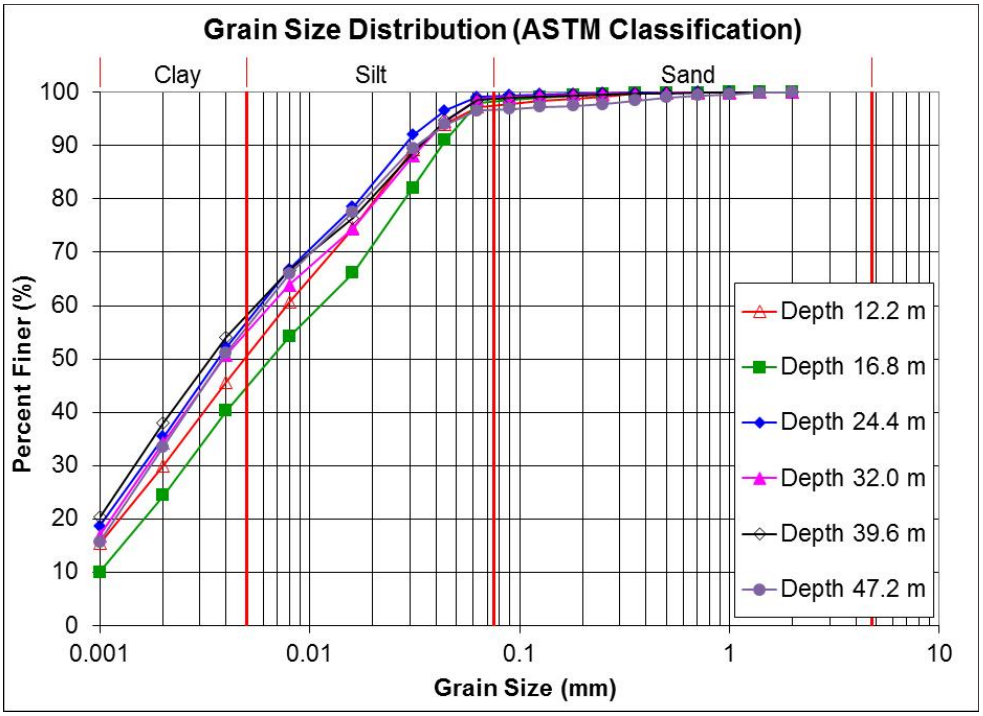

Fig. 6. Gradation chart of soil samples from BH150316

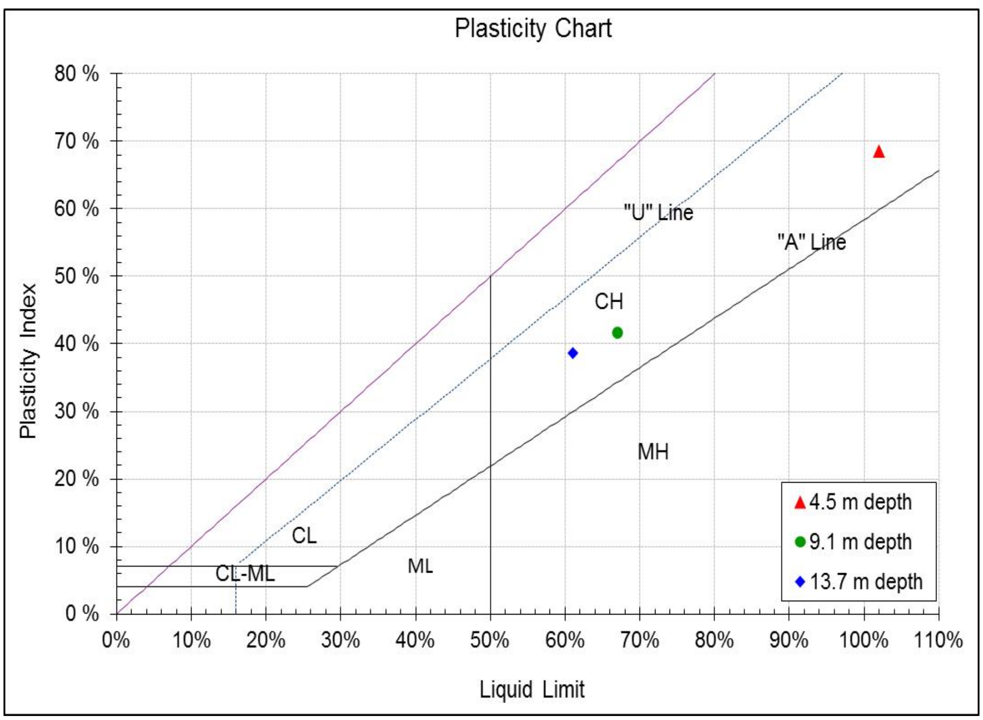

Fig. 7. Plasticity chart of soil samples from BH140924

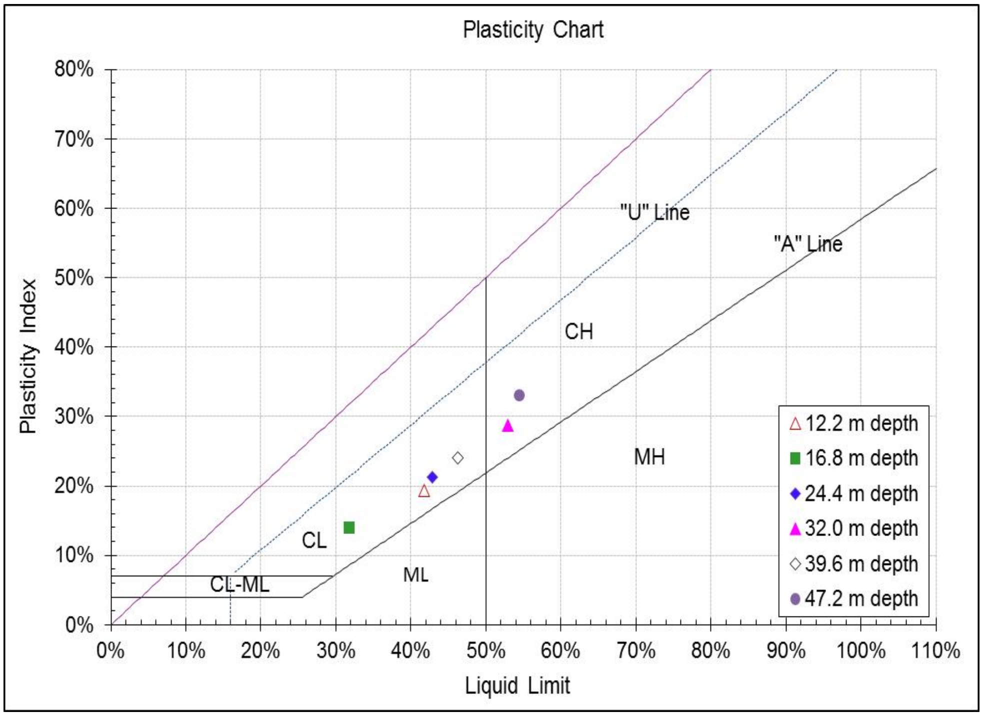

Fig. 8. Plasticity chart of soil samples from BH150316

As seen from Table 2, Fig. 5 and Fig. 7, the samples from BH140924 are clay to silty clay of high to extremely high plasticity. The plasticity index ranges from 38.6% to 68.6%. The natural moisture contents are higher than the liquid limits for all the samples collected from BH140924.

The gradation chart for BH150316 (Fig. 6) shows the soil samples as silty clay or clayey silt. The fine sediments at this site have higher silt content compared to the other site (BH140924). The soil plasticity index ranges from 13.9% to 33%. The soils exhibit low to high plasticity. As shown in the borehole log (Appendix A), the clay/silt materials above 30 m depth had moisture content higher than the liquid limit.

The unconfined undrained shear strength results from the pocket penetrometer tests are discussed along with the VST and CPT data below.

4.3 VST Results and CPT Data Calibration

The peak and remolded undrained shear strengths from the VST at both BH140924 and BH150316 are provided in the borehole logs in Appendix A. The CPT plots of corrected tip resistance (q_t), sleeve friction (f_s), friction ratio (R_f), the dynamic pore pressure (u_2), the interpreted Soil Behaviour Types, and the pore pressure dissipation test results are provided in Appendix B.

The VST results are used to calibrate the CPT data. The soil undrained shear strength (S_u) is conventionally calculated from the CPT tip resistance as follows:

$$S_u = (q_t - \sigma_{vo}) / N_{kt} \qquad (5)$$

where q_t is the total corrected cone tip resistance as calculated using Eq. 3;
σ_{vo} is the total vertical overburden stress;
N_{kt} is a bearing factor (Konrad & Law, 1987; Yu & Mitchell, 1998).

The S_u value can also be independently calculated entirely from the excess pore water pressure measurements (Δu) as follows:

$$S_u = \Delta u / N_{\Delta u} \quad (6)$$

where Δu is commonly determined from $\Delta u = (u_2 - u_{eq})$ with u_2 being the recorded dynamic pore pressure behind the tip of the cone (shoulder element); u_{eq} is the equilibrium pore pressure determined from water table depth; and
$N_{\Delta u}$ is a pore pressure bearing factor (Tavenas & Leroueil, 1987).

Note that N_{kt} and $N_{\Delta u}$ are linked as:

$$N_{\Delta u} = B_q\, N_{kt} \quad (7)$$

where B_q is a pore pressure parameter determined as follows:

$$B_q = (u_2 - u_{eq})/(q_t - \sigma_{vo}) \quad (8)$$

By comparing the VST and CPT data at CPT-01, the bearing factors are determined to be $N_{kt} = 11.5$ and $N_{\Delta u} = 9.8$ for this location. The average B_q is 0.85 at CPT-01. The S_u and B_q profiles for CPT-01 are shown in Fig. 9. Similar results were obtained at CPT-01A as shown later and in Appendix B. Note that Wang et al. (2015) presented $N_{kt} = 10.5$, $N_{\Delta u} = 11$ and $B_q = 1.05$. An update of the data was received from the drilling contractor after the paper was published. The information provided in this Open File represents the latest update.

The field vane shear tests at CPT-04 allowed further calibration of the CPT data. By comparing the VST and CPT data at CPT-04, it was found that the bearing factor N_{kt} remains the same as that determined from CPT-01, i.e., $N_{kt} = 11.5$, but $N_{\Delta u}$ changed to 8.1. Note that the average B_q of CPT-04 is 0.7 (Fig. 10). The $N_{\Delta u}$ =8.1 is the product of the average B_q and N_{kt} (Eq. 7). The calibrated CPT $S_u(N_{kt})$ and $S_u(N_{\Delta u})$ are given in Fig. 10.

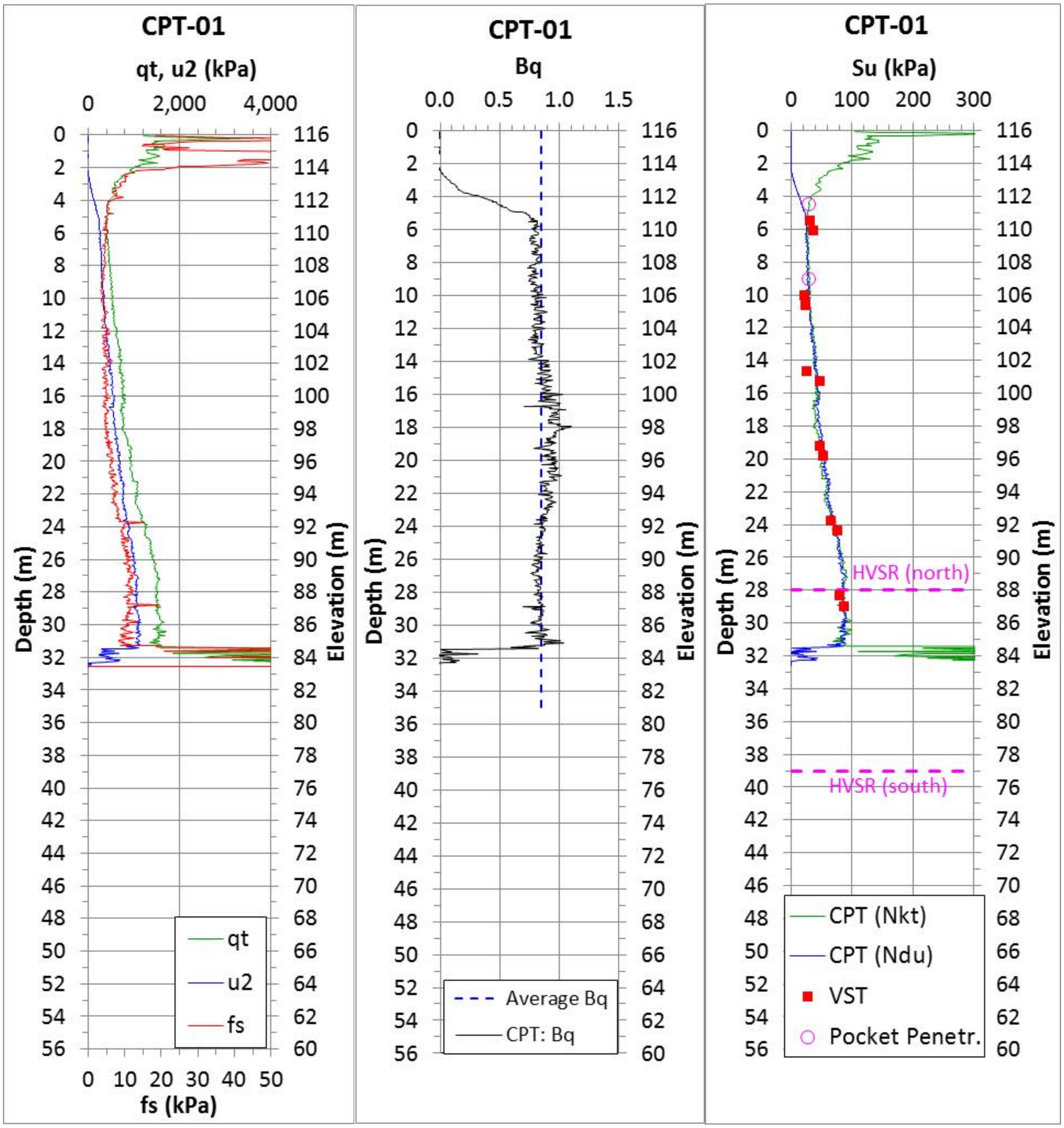

Fig. 9. CPT-01 test results and calibration

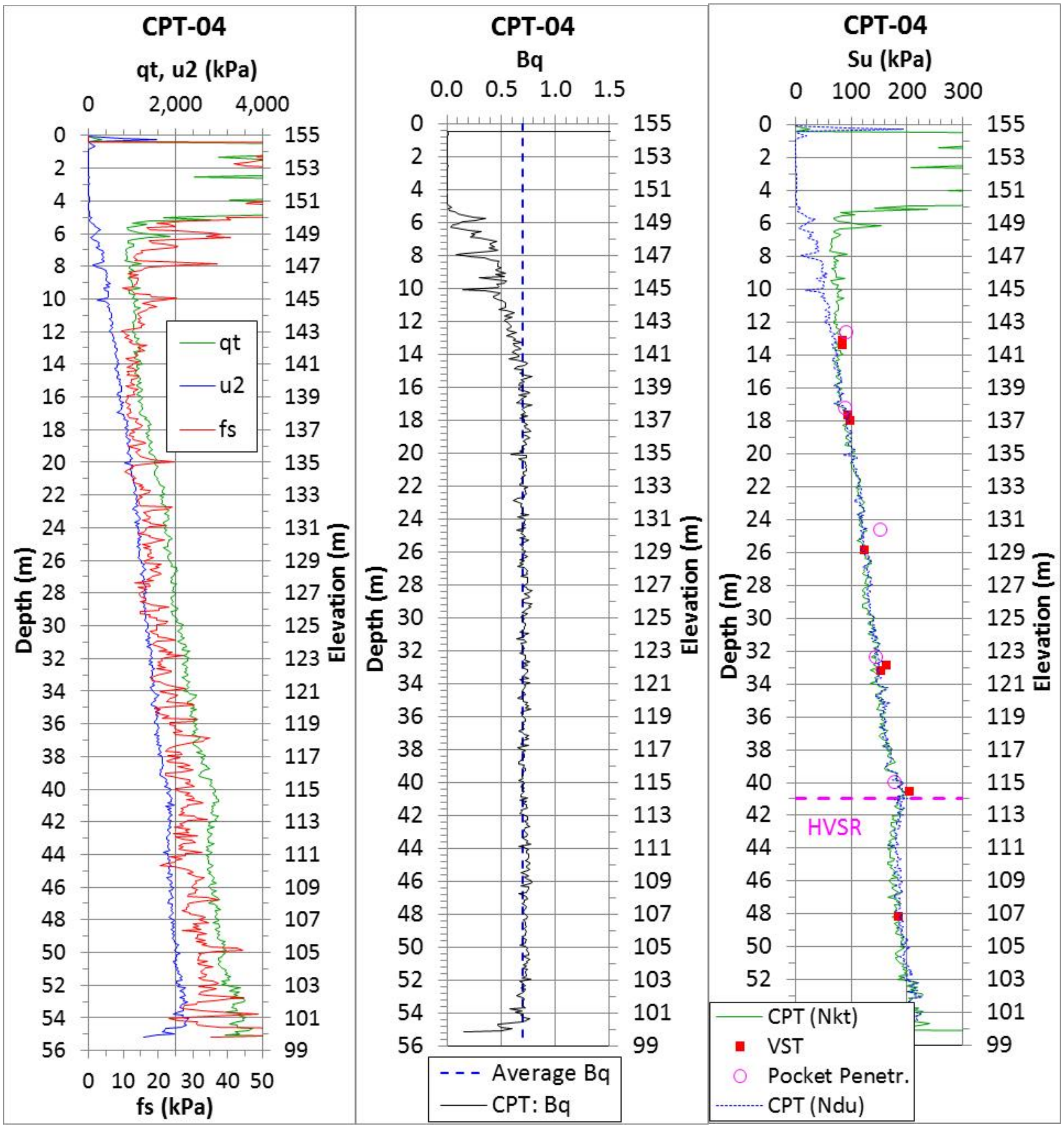

Fig. 10. CPT-04 test results and calibration

The unconfined undrained shear strength results from the pocket penetrometer tests on the Shelby samples are also presented in Figs. 9 and 10. As shown in these figures, the pocket penetrometer test results are reasonably close to the confined undrained shear strength from the VST and the CPT. The pocket penetrometer can therefore be a useful tool for quick undrained shear strength tests in the field where clays are accessible.

4.4 Shear Strength Results at All CPT Locations

Based on the above data calibration, the soil undrained shear strengths at all CPT locations are calculated with N_{kt} = 11.5. Eq. 7 was used to determine $N_{\Delta u}$ for each of the CPT locations. An average B_q value was used at each CPT site. The B_q profiles and the average values are shown in Fig. 11. The interpreted $S_u(N_{kt})$ and $S_u(N_{\Delta u})$ values for all the CPTs are shown in Fig. 12. The $S_u(N_{\Delta u})$ profiles so interpreted are reasonably close to the $S_u(N_{kt})$ profiles.

It should be noted that ground water tables shown on the CPT plots in Appendix B were determined based on the pore pressure dissipation tests at each CPT location except for CPT-01 (and CPT-01A) where the water table was assumed. A dissipation test was done at 31.85 m depth at CPT-01 where a higher permeability unit (overlying bedrock) was encountered. The hydraulic head right above the bedrock was 22 m high (at 31.85 m depth) or 9.85 m below surface. However, laboratory tests of soil samples (Appendix A) indicated that the soils at 5 m depth and below were fully saturated. The lower hydraulic head near bedrock was probably attributed to the dynamic effect of the sloping topography towards the west (Fig. 1) as well as the westward dipping bedrock (Fig. 4). Artesian wells were available in the farm field down slope to the west. Artesian pressure was measured further to the west at CPT-02. The 31 m thick low permeability clay overburden may have had a “damping” effect on the dynamics of the hydraulic head near bedrock. The water table at CPT-01 was therefore assumed to be at 5 m depth based on the soil moisture measurements.

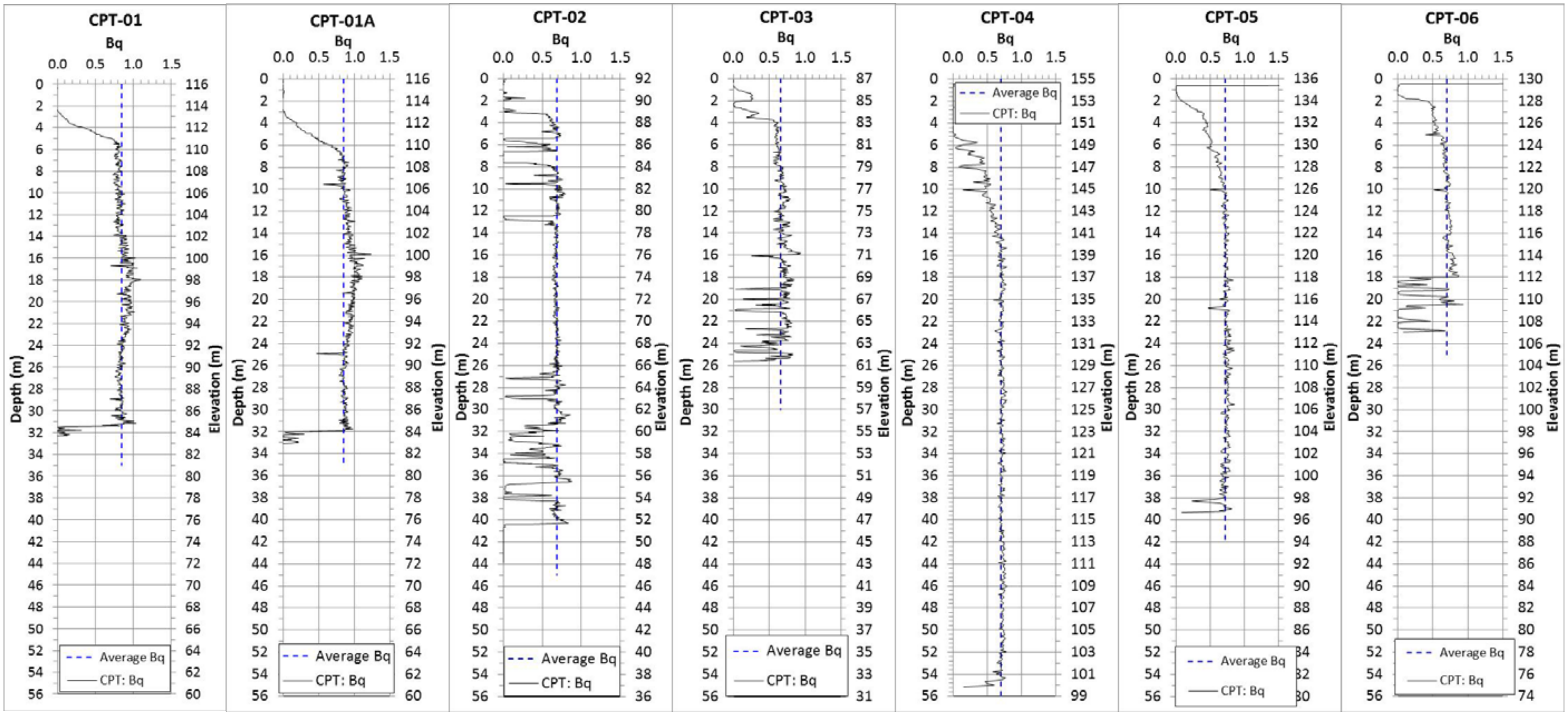

Fig. 11. Profiles of pore water pressure parameter B_q at CPT-01 through CPT-06

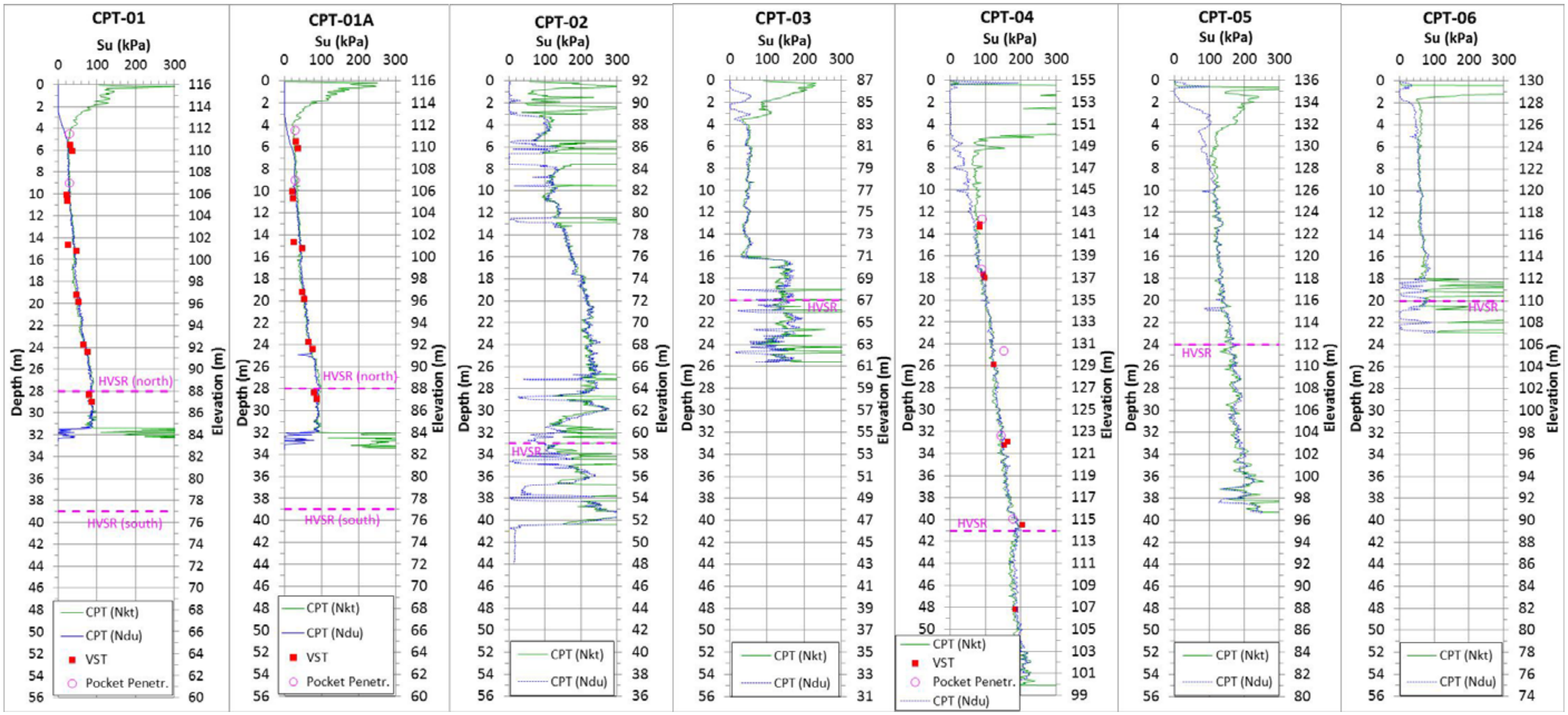

Fig. 12. Undrained shear strength at CPT-01 through CPT-06

4.5 Shear Wave Velocities from Seismic Cone Measurements at CPT-04

Shear wave velocities (V_s) were measured at 1 m depth interval at CPT-04. Fig. 13 shows the interval results. Discussions of the results are provided in the next section.

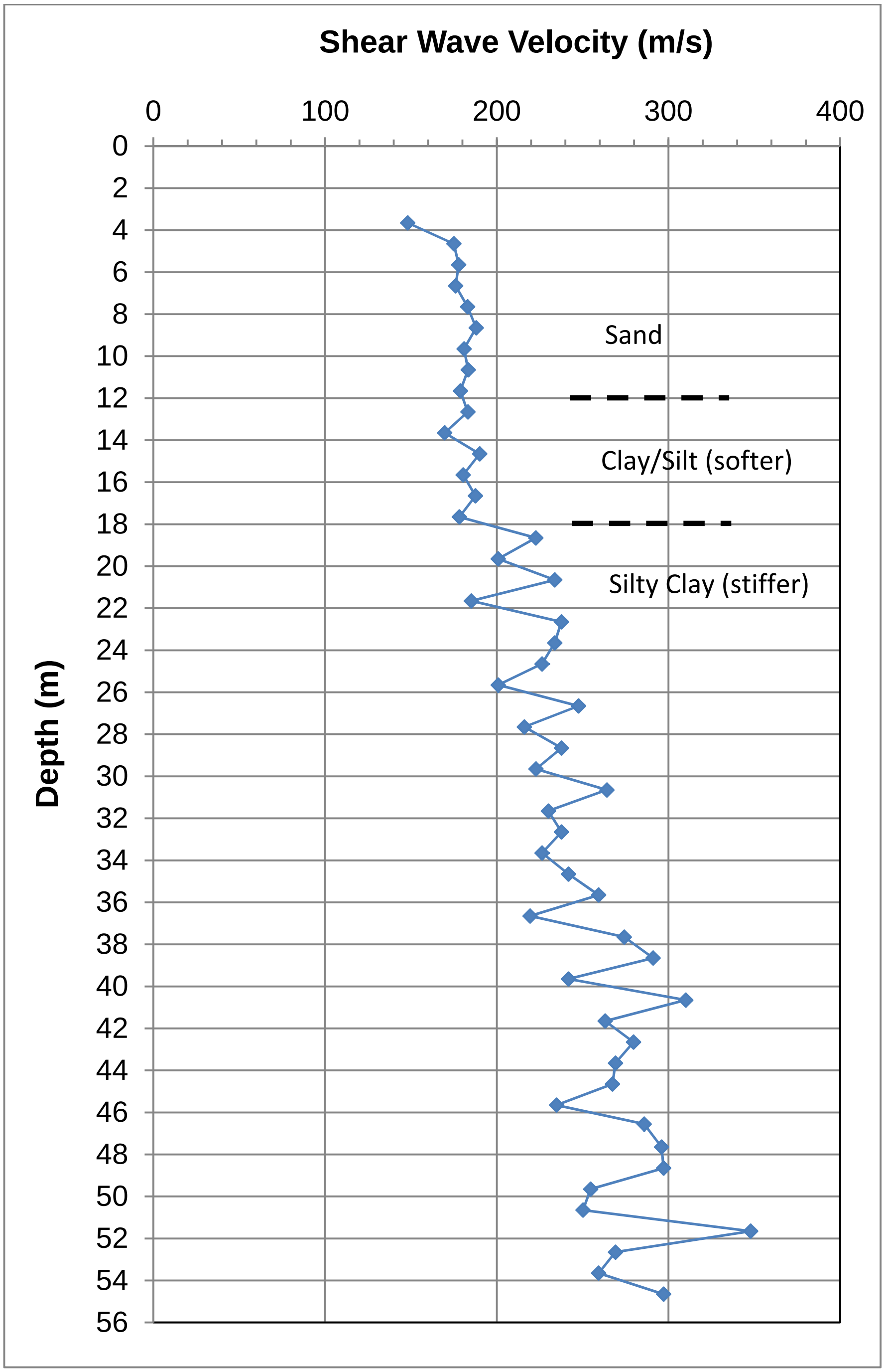

Fig. 13. Interval shear wave velocities measured at CPT-04

5. INTERPRETATION AND DISCUSSION

5.1 Undisturbed Sites Outside the Landslide Scar

CPT-01, 01A, 04 and 06 are in the undisturbed area outside the landslide scar. The results from the repeat test at CPT-01A are very similar to that of CPT-01 (Figs. 11, 12 and Appendix B).

Based on the CPT soil behaviour type, the materials at CPT-01 from the surface down are inferred to as: 0 to 3 m - clay/silt; 3 to 21 m - sensitive clay; 21 to 31 m - silt of increased stiffness; 31 m to 33 m - sandy/clayey silt; and 33 m depth - refusal (bedrock). The undrained shear strength ranged from 22 kPa to about 90 kPa increasing with depth approximately linearly. The HVSR measurement at 340 m north of CPT-01 indicates a depth to impedance of 28 m. Another HVSR measurement at about 70 m south of CPT-01 interprets an impedance depth of 39 m. The CPT bedrock depth of 33 m falls within the HVSR interpretations of 28 m and 39 m which is a reasonable confirmation of the HVSR survey results.

CPT-06 is across the Quyon River from CPT-01 (Fig. 1). It is on the crest of the west scarp of the landslide. The soil behaved similarly to that of CPT-01. The CPT soil behaviour types are, from surface down, 2 m sand, 16 m clay, 5 m silty sand and then bedrock. The undrained shear strength of the clay material ranged from about 60 to 80 kPa. Although the strength is slightly higher than that of similar depth at CPT-01, it is agreeable with that of the lower depth at CPT-01. The HVSR impedance depth at this location is 20 m. The CPT sounding of the clay bottom is at 18 m and bedrock (refusal) at 23 m depth, which confirmed the HVSR impedance measurement.

CPT-04 (and BH150316) is about 85 m north of the head scarp of the landslide zone (Fig. 1). Fine sand was encountered from surface to 12.2 m depth. A 10 cm sand cap was observed at the top of the clay core collected from 12.2 m depth. The CPT non-normalized Soil Behaviour Type indicated a material change at 12.0 m depth (Appendix B), which is consistent with the observations from the drill cuttings and the Selby sample. The CPT indicated a continuous S_u profile below 12 m depth (Fig. 10). The S_u values at this site are higher than that of the southern sites (CPT-01 and CPT-06). The upper clay/silt layer (above 18 m depth) has a shear strength lower than 100 kPa. It increased up to 200 kPa at 41 m depth. The S_u profile changed at 41 m depth with the gradient decreased slightly. Coincidentally, the HVSR measurement at this location detected impedance at 41 m depth. However, the HVSR impedance is 14 m above the bedrock. It is suspected that this might have been attributed to the sloping or irregular bedrock surface (note outcrop about 800 m southwest of CPT-04 in Fig. 1).

The shear wave velocity profile (Fig. 13) measured at CPT-04 is consistent with the borehole observations and the CPT measurements. A nearly constant interval V_s of approximately 180 m/s was measured from 4 m to 12 m depth where the sand unit was observed. Similar V_s was measured from 12 m to 18 m depth but with somewhat different signatures (slightly increased value and variation). The low V_s corresponds to the low strength measured by the CPT (Fig. 10). The V_s increased linearly below 18 m depth. The increase slowed down below 41 m depth, which is consistent with the S_u profile shown in Fig. 10.

5.2 Disturbed Sites inside the Landslide Scar

CPT-02, 03 and 05 are located inside the landslide disturbed area. CPT-02 is about half way between CPT-01 and CPT-06 (Fig. 1). It is near the centre (or bottom) of the Quyon River valley. The undrained shear strength ranged from about 100 to 250 kPa (Fig. 12). The continuous low strength clay unit observed from CPT-01 and CPT-06 is absent at CPT-02. This is likely the result of the landslide where the low strength sensitive clay was disturbed and displaced. The disturbance is observed from the S_u profile of the upper 12 m in Fig. 12. The S_u discontinuity in this upper zone is not observed in the undisturbed locations (CPT-01, CPT-04 and CPT-06). The disturbance is consistent with the observations along the nearby Quyon River where exposed clays exhibit tilted and noticeably displaced beds at similar elevation. The continuous S_u profile below 12 m depth is an indication that the stronger material has probably remained undisturbed. The landslide slip surface is therefore likely at 10 ±3 m depth at CPT-02, which is around the elevation of the nearby Quyon River.

The HVSR impedance depth measured at CPT-02 is 33 m. Note that an extremely hard layer (see q_t chart in Appendix B) was encountered at 32 to 33 m depth. The HVSR impedance depth corresponds to this layer.

CPT-03 is near the centre of the Quyon River valley and located at about 1.8 km downstream of CPT-02. The CPT detected a softer unit of S_u ranging from 30 to 50 kPa between 4 and 16 m depth (Fig. 12). There is a sharp strength change at 16 m depth where the shear strength increases abruptly by about 100 kPa. Refusal (bedrock) was encountered at 25.7 m depth. The abrupt soil profile change is inconsistent with the soil profiles obtained from the undisturbed sites (CPT-01, CPT-01A and CPT-06). It is therefore likely that the landslide slip surface is at 16 m depth at CPT-03.

Several HVSR impedance measurements in the vicinity of CPT-03 consistently indicate an interface depth of 20 m. This falls in the hard layer between 16 m and 25.7 m depth overlying the bedrock (refusal), which is a fairly reasonable confirmation of the HVSR measurements.

CPT-05 is about 1.8 km downstream of CPT-04. The surface elevation at CPT-05 dropped by 19 m compared to CPT-04. As seen in Fig. 12, a continuous S_u profile was detected at CPT-05. This is similar to that of CPT-04. However, the softer unit of S_u less than 100 kPa is absent from CPT-05. The $S_u(N_{kt})$ values at this site ranged from 120 kPa to 250 kPa. By comparing with CPT-04, the continuous S_u profile below the 7 or 8 m depth at CPT-05 indicates that the materials might be undisturbed. The absence of the softer unit above is an indication that the landslide might have removed this upper layer at this location. The elevation at the 8 m depth at CPT-05 is 128 m asl. According to the borehole and laboratory results from BH150316 (Appendix A), the moisture contents of the undisturbed clay above 128 m elevation were higher than the liquid limit. This is additional evidence that the upper clay layer flowed away during the landslide.

The HVSR impedance depth is 24 m at CPT-05, which is about 15 m above the bedrock. This is similar to the measurement at CPT-04 where the HVSR impedance is at 14 m above the bedrock. Again, it is suspected that sloping or irregular bedrock surface might be the cause of the shallower impedance. Note that dramatic rock elevation change is visible along the Quyon River about 400 m to the east of CPT-05, where a waterfall developed across a bedrock outcrop.

9. CONCLUSIONS

Resonance mapping using the HVSR technique indicates a bedrock valley underlying the landslide. Depths to the HVSR impedance boundary were calculated using a region-specific depth function developed by Hunter et al (2010). At sites CPT-01, 02, 03, and 06, the impedance depths are in agreement with the CPT observations within the error range provided by the empirical correlation (±6.1 m). Where the estimated depth did not agree suggests that bedrock is sloping underneath the site, which is evident from the nearby outcrops.

The CPT data were calibrated with VST results obtained from two drill hole locations in the undisturbed areas outside the landslide scar. The calibration indicated a constant CPT bearing factor of N_{kt} = 11.5. The pore pressure bearing factor $N_{\Delta u}$ varies by site. An average B_q value at each CPT location was used to determine $N_{\Delta u}$ that resulted in S_u profiles similar to that calculated from N_{kt}.

A clay unit of continuous S_u profile was detected from all the CPT holes at the undisturbed locations outside the landslide scar (CPT-01, CPT-04 and CPT-06). Materials of S_u less than 100 kPa exist at all the undisturbed locations tested. This lower strength is consistent with the lower shear wave velocity measured at CPT-04.

The laboratory tests identified the materials from boreholes BH140924 (near CPT-01) and BH150316 (near CPT-04) as clay to silty clay or clayey silt. The materials from the southern site are finer and softer than that of the northern site. The clay materials at the southern site exhibit high to extremely high plasticity. Those from the northern site have low to high plasticity. The samples collected from depth shallower than 30 m at both the northern and southern sites have natural moisture content higher than their liquid limit.

The results of the pocket penetrometer tests on the soil samples from both BH140924 and BH150316 agree well with the VST and CPT data.

Three CPT holes were drilled inside the landslide disturbed zone (CPT-02, CPT-03 and CPT-05). The material with S_u less than 100 kPa was not found from CPT-02 and CPT-05, which indicates that the softer materials have been displaced by the landslide. The continuous shear strength profiles at lower elevations in these test holes suggest that the materials are likely undisturbed by the landslide. Although a softer unit was detected at CPT-03, an abrupt S_u profile change is inconsistent with those found from the undisturbed locations. It is therefore an indication that the upper softer material was likely moved to this location by landslide.

ACKNOWLEDGEMENT

The authors would like to thank Alain Grenier, Matthew DeGeer, Andrea Reman, and Aldo Katrigjini for their kind assistance in the field. Kind support from Heather Crow has been critical on obtaining funds and access to summer students for the field work. The authors would also like to thank Heather Crow and Didier Perret for their input throughout the project. Their review helped considerably on the improvement of the manuscript. This report is a product of the Public Safety Geoscience Program of the Earth Sciences Sector (ESS), Earthquake Geohazard Project, Natural Resources Canada.

REFERENCE

Adams J., Basham, P., 1989. The seismicity and seismotectonics of Canada east of the Cordillera. Geoscience Canada 16, 3-16.

Adams J., Basham, P., 1991. The seismicity and seismotectonics of eastern Canada. In: Slemmons, D.B., Engdahl, E.R., Zoback, M.D., Blackwell, D.D., (eds.), Neotectonics of North America. Geological Society of America, Decade Map Volume 1, pp. 261-276.

Aylsworth, J.M., Lawrence, D.E., Evans, S.G., 1997. Landslide and settlement problems in sensitive marine clay, Ottawa Valley: field trip B1 guidebook. Ottawa '97, Geological Association of Canada, Mineralogical Association of Canada, Ottawa.

Basham, P.W., Weichert, D.H., Anglin, F.M., Berry, M.J., 1982. New probabilistic strong ground motion maps of Canada: a compilation of earthquake source zones, methods and results. *Earth Physics Branch, Open File 82-33*.

Brooks, G.R., 2013. A massive sensitive clay landslide, Quyon Valley, southwestern Quebec, Canada, and evidence for a paleoearthquake triggering mechanism. Quaternary Research, 80, 425-434.
Dyke and Prest, 1987

Brooks, G.R., B.E. Medioli, J.M. Aylsworth & D.E. Lawrence, 2004. A compilation of radiocarbon dates relating to the age of sensitive clay landslides in the Ottawa Valley, Ontario-Quebec, *Geological Survey of Canada, Open File 7432*, 58 p.

Dobry, R., Oweis, I. and Urzua, A., 1976. Simplified procedures for estimating the fundamental period of a soil profile, Bull. Seismol. Soc. Am. 66, 1293–321.

Dyke, A.S., Prest, V.K., 1987. Late Wisconsinan and Holocene history of the Laurentide Ice Sheet. Géographie Physique et Quaternaire 41, 237–263.

Fransham, P.B., Gadd, N.R., Carr, P.A., 1976. Sensitive clay deposits and associated landslides in Ottawa Valley. Geological Survey of Canada, Open File 352.

Gadd, N.R., 1986. Lithofacies of Leda clay in the Ottawa basin of the Champlain Sea. Geological Survey of Canada, Paper 85-21.

Gadd, N.R., 1987. Geological setting and Quaternary deposits of the Ottawa Region. In: Fulton, R.J. (Ed.), Quaternary geology of the Ottawa region, Ontario and Quebec. Geological Survey of Canada, Paper, 86-23, pp. 3–9.

Hunter, J. A., H. Crow, G. R. Brooks, M. Pyne, M. Lamontagne, A. Pugin, S. E. Pullan, T. Cartwright, M. Douma, R. A. Burns, R. L. Good, D. Motazedian, K. Kaheshi-Banab, R. Caron, M. Kolaj, I. Folahan, L. Dixon, K. Dion, A. Duxbury, A. Landriault, V. Ter-Emmanuil, A. Jones, G. Plastow, and D. Muir 2010. Seismic site classification and site period mapping in the Ottawa area using geophysical methods, Geol. Surv. Can., Open-File Rept. 6273.

Hunter, J.A. and Crow, H.L. (ed.), 2012. Shear wave velocity measurement guidelines for Canadian seismic site characterization in soil and rock; Geological Survey of Canada, Open File 7078, 227p. doi: 10.4095/291753.

Keefer, D.K., 1984. Landslides caused by earthquakes: Geological Society of America Bulletin 95, 406-421.

Konrad, J.M. and Law, K.T. 1987. Undrained shear strength from piezocone tests. Canadian Geotechnical Journal, 24 (3): 392-405.

Kramer, S. L., 1996. Geotechnical Earthquake Engineering, Prentice Hall, New Jersey, 653p.

Lajoie, P.G., 1962. Soil Survey of Gatineau and Pontiac Counties. Research Branch, Canada Department of Agriculture, Ottawa.

Lamontagne, M., 2010. Historical earthquake damage in the Ottawa-Gatineau region, Canada. Seismological Research Letters 81, 129-139.

National Research Council of Canada (NRCC), 2010. National Building Code of Canada, ISBN 0-660-19975-7.

Richard, R.H., 1976. Surficial Geology, Quyon, Quebec–Ontario, Geological Survey of Canada, Open File 363.

Robertson, P.K., Campanella, R.G., Gillespie, D. and Greig, J., 1986, "Use of Piezometer Cone Data", Proceedings of InSitu 86, ASCE Specialty Conference, Blacksburg, Virginia.

Robertson, P.K., 1990, "Soil Classification Using the Cone Penetration Test", Canadian Geotechnical Journal, Volume 27: 151-158.

Robertson, P.K., 2009, "Interpretation of cone penetration tests – a unified approach", Canadian Geotechnical Journal, Volume 46: 1337-1355.

Rodríguez, C.E., Bommer, J.J., Chandler, R.J., 1999. Earthquake-induced landslides: 1980–1997. Soil Dynamics and Earthquake Engineering 18, 325–346.

St.-Onge, D.A., 2009. Surficial geology, lower Ottawa Valley, Ontario–Quebec. Geological Survey of Canada, A Series Map 2140A.

Tavenas, F. and Leroueil, S., 1987. State-of-the-art on laboratory and in-situ stress-strain-time behavior of soft clays. Proc. International Symposium on Geotechnical Engineering of Soft Soils, Mexico City: 1-146.

Wang, B., G.R. Brooks and J.A.M. Hunter, 2015. Geotechnical investigations of a large landslide site at Quyon, Québec. Proc. of the 68th Canadian Geotechnical Conference, GéoQuébec2015, Québec, Sept. 20-23, 2015.

Wilson, M.E., 1924. Arnprior-Quyon and Maniwaki areas Ontario and Quebec. Geological Survey of Canada, Memoir 136.

Yu, H.S. and Mitchell, J.K., 1998. Analysis of cone resistance: review of methods. Journal of Geotechnical and Geoenvironmental Engineering, 124 (2): 140-149.

Appendix A

Borehole Logs

Borehole#	BH140924	Coord.: N45º33'24.7" W76º15'41.3'	Site: Alexander Road near 6th Concession, Quyon, QC (~15 m east of CPT-01)
Drill Date:	2014-09-24	Datum: WGS 84	Equipment/Instrument: Auger OD 165, ID 83; Shelby ID 70, OD 73, L 676 (mm)
Drill Type:	H.S. Auger	UTM Zone: 18 (78º-72ºW)	Drilling Contractor: OGS Inc.

Depth (m)	Elev (m)	Samp. #	Symb.	Description of Materials	Instr. Detail	W_c (%)	PL (%)	LL (%)	I_p (%)	γ (kN/m³)	G_s	Grain Size	S_u (kPa)	S_{ur} (kPa)	Notes
0	116														
1	115														
2	114														
3	113														
4	112														
			X	CLAY, grey	§						2.74		29.4		4.5m: Shelby core
5	111			at 5m: alternating ~2cm brownish		108.7	33.4	102.0	68.6	14.4	2.74	X			\ pocket penetr. tests on core
				layers every 10 cm.	+						2.77		30.8	8.4	5.5m: Field VST (NW-vane)
6	110			Samples: M030, M126, M086, M137,	+								36.4	8.4	6.1m: Field VST
				M100, M139, M125, M404, M107											
7	109														
8	108														
9	107		X	CLAY, grey	§	79.3	25.5	67.0	41.5		2.77		28.6		9.1m: Shelby core
				Samples: M041, M080, M027, M066,						14.6	2.74	X			\ pocket penetr. tests on core
10	106			M123, M005, M033, M058, M013,	+						2.74		22.4	9.8	10.1m: Field VST
				M142	+								23.8	5.6	10.7m: Field VST
11	105														
12	104														
13	103														
			X	CLAY, grey		67.3	22.5	61.1	38.6	15.8	2.75	X			13.7m: Shelby core
14	102			Samples: M053, M117, M028, M085,							2.77				Lower 30cm core lost
				M129, M149 (disturbed)	+								25.2	11.2	14.6m: Field VST
15	101				+								47.6	16.8	15.2m: Field VST
16	100														
17	99														
18	98														18m: Shelby core lost
19	97				+								47.6	22.4	19.2m: Field VST
					+								53.1	25.2	19.8m: Field VST
20	96														
21	95														
22	94														
23	93														23m: Shelby core lost
24	92				+								64.3	22.4	23.8m: Field VST
					+								75.5	30.8	24.4m: Field VST
25	91			***Legend:***											
				§ Pocket penetrometer test											
26	90			*+ Vane shear test*											
27	89														
															27.5m: Shelby core lost
28	88														
					+								79.7	36.4	28.4m: Field VST
29	87			End of borehole at 29.5 m depth	+								86.7	30.8	29.0m: Field VST

Geological Survey of Canada	Project: PSG/Intraplate EQ/PaleoEQ
Natural Resources Canada	Logged by: Baolin Wang
Note: Surface elevation from LiDAR data	

Fig. A-1. Borehole log and lab results of BH140924. (W_c = water content; PL = plastic limit; LL = liquid limit; I_p = plasticity index; γ = unit weight; G_s = specific gravity; S_u = undrained shear strength; S_{ur} = remolded undrained shear strength)

Borehole#	BH150316	Coord.: N45º36'07.2" W76º21'47.7"	Site:	19 - 8th Line Road, Bristol, QC (~10m south of CPT-04)
Drill Date:	2015-03-16	Datum: WGS 84	Equipment/Instrument:	Auger OD 165, ID 83; Shelby ID 70, OD 73, L 676 (mm)
Drill Type:	H.S. Auger	UTM Zone: 18 (78º-72ºW)	Drilling Contractor:	CCC Geotechnical and Environmental Drilling Ltd.

Depth (m)	Elev (m)	Samp. #	Symb.	Description of Materials	Instr. Detail	W_c (%)	PL (%)	LL (%)	I_p (%)	γ (kN/m^3)	G_s	Grain Size	S_u (kPa)	S_{ur} (kPa)	Notes
0	155			SAND, fine, uniform, grey											
1	154														
2	153														
3	152														
4	151														
5	150														
6	149														
7	148														
8	147														
9	146														
10	145														
11	144														
12	143		X	CLAY/SILT, grey	§	45.9	22.4	41.8	19.4	17.0	2.79	X	90.3		12.2m: Shelby sample.
				Samples: M015, M111, M187, M077,	+								84.5	16.4	VST: N-type vane.
13	142			M070, M069, M084, M038, M403,	+								84.5	11.7	VST: N-type vane.
				M120, M039, M436, M135											
14	141														
15	140														
16	139														
			X	SILT, clayey, grey	§	37.6	18.0	31.9	13.9	18.0	2.78	X	89.1		16.8m: Shelby core
17	138			Samples: M060, M103, M092, M133,	+								93.9	21.1	
				M020, M408, M079, M017, M420,	+								96.3	16.4	
18	137			M113, #176											
19	136														
20	135														
21	134														
22	133														
23	132														
24	131		X	CLAY, silty, grey	§	45.4	21.6	42.9	21.3	17.2	2.78	X	152.2		24.4m: Shelby core
				Samples: M057, M114, M131, M147,	+										Large sized vane didn't
25	130			M052, M083, M012, M072, M115,	+										shear at 50 lb-ft torque
				M056, M062	+								123.5	61.7	limit. Changed to smaller
26	129														vane.
27	128														
28	127														
29	126														
30	125														
31	124														
32	123		X	CLAY, silty, grey	§	47.3	22.2	53.0	28.8	17.0	2.78	X	143.9		32.0m: Shelby core
				Samples: M096, M009, M099, M074,	+								164.6	66.9	
33	122			M019, M410	+								154.3	51.4	
34	121														

35	120																
36	119																
37	118																
38	117																
39	116																
			X	CLAY, silty, grey	§			40.8	22.2	46.3	24.1	17.7	2.78	X	178.1		39.6m: Shelby core
40	115			Samples: M048, M145, M411, M122,	+										205.8	77.2	Su at approx. ASTM limit.
				M146	+												Su much exceeded ASTM
41	114																200 kPa limit. Discarded.
42	113																
43	112																
44	111																
45	110																
46	109																
47	108		X	CLAY, silty, grey	§			40.2	21.5	54.5	33.0	17.8	2.78	X			47.2m: Shelby core
				Samples: M050, M105, M150, M118,	+										185.2	66.9	\Sample cracked on pocket
48	107			M435, M124, M128	+												penetrometer test.
				End of borehole at 48.5m depth.													\Su much exceeded ASTM
49	106																200 kPa limit. Discarded.
50	105																**Legend:**
																	§ Pocket penetrometer test
51	104																+ Vane shear test

Geological Survey of Canada	Project:	PSG/Intraplate EQ/PaleoEQ
Natural Resources Canada	Logged by:	Baolin Wang
Note: Surface elevation from LiDAR data		

Fig. A-2. Borehole log and lab results of BH150316. (W_c = water content; PL = plastic limit; LL = liquid limit; I_p = plasticity index; γ = unit weight; G_s = specific gravity; S_u = undrained shear strength; S_{ur} = remolded undrained shear strength)

APPENDIX B

Cone Penetrometer Test Results

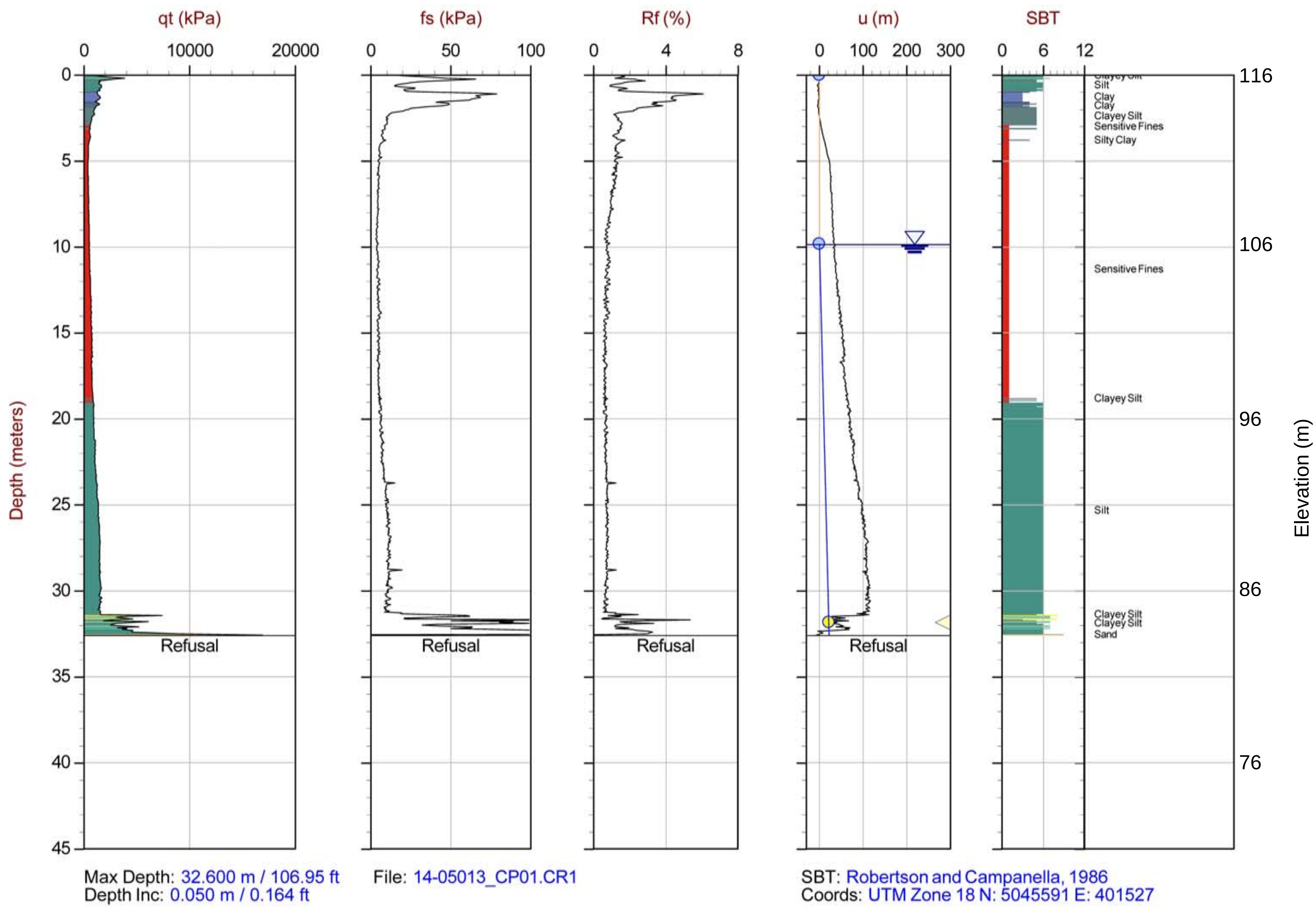

Fig. B-1. Non-normalized Plots – CPT-01

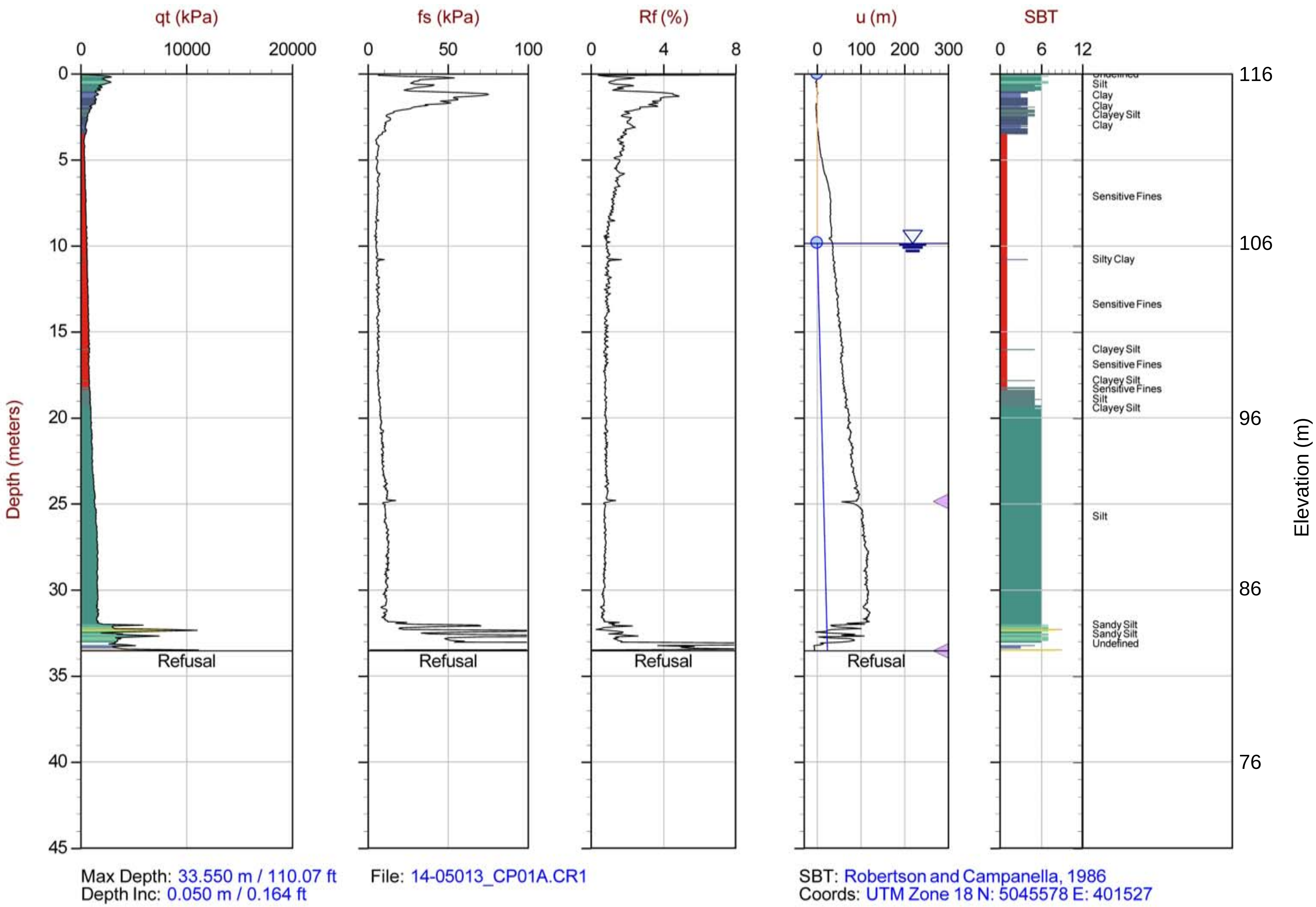

Fig. B-2. Non-normalized Plots – CPT-01A

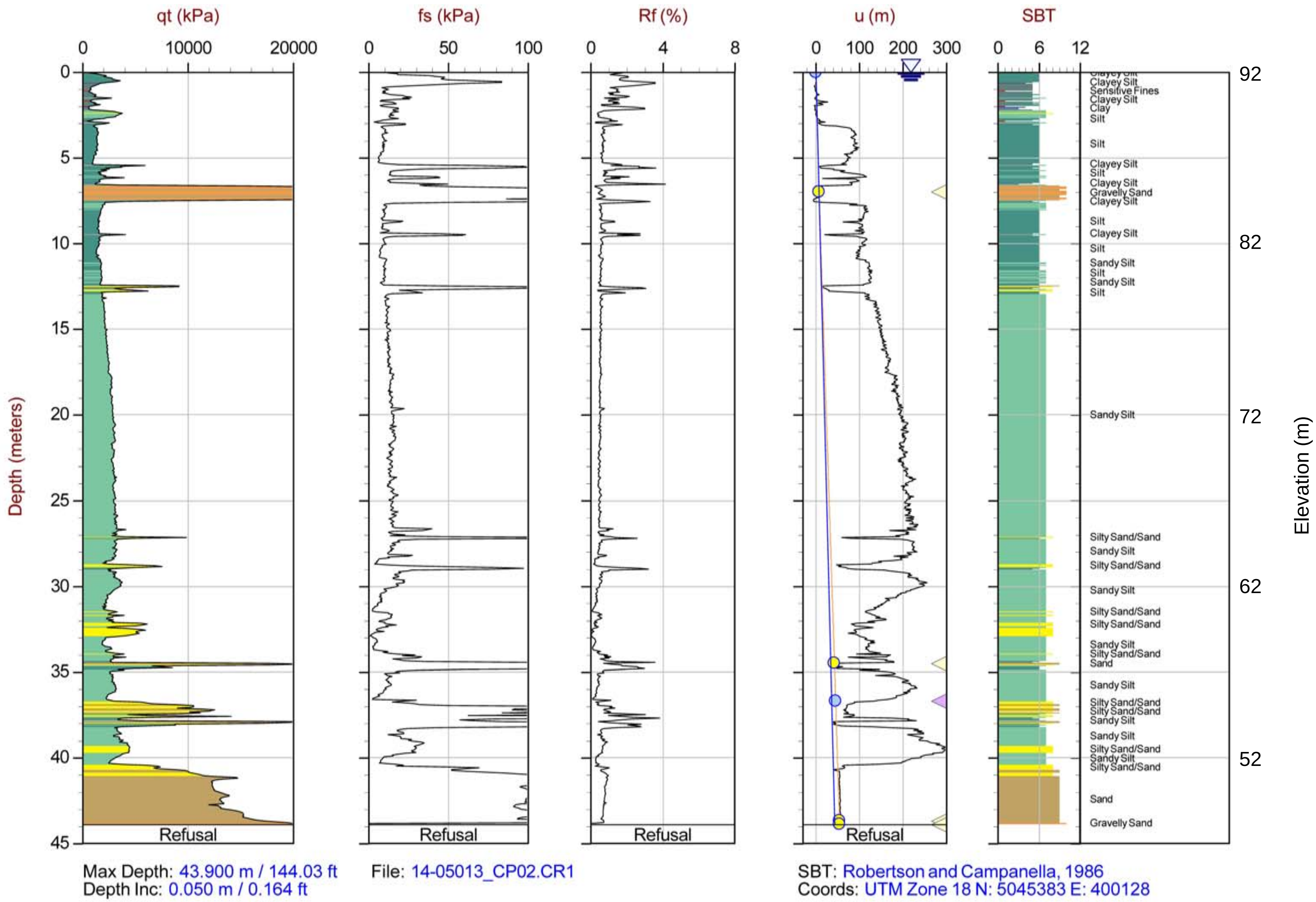

Fig. B-3. Non-normalized Plots – CPT-02

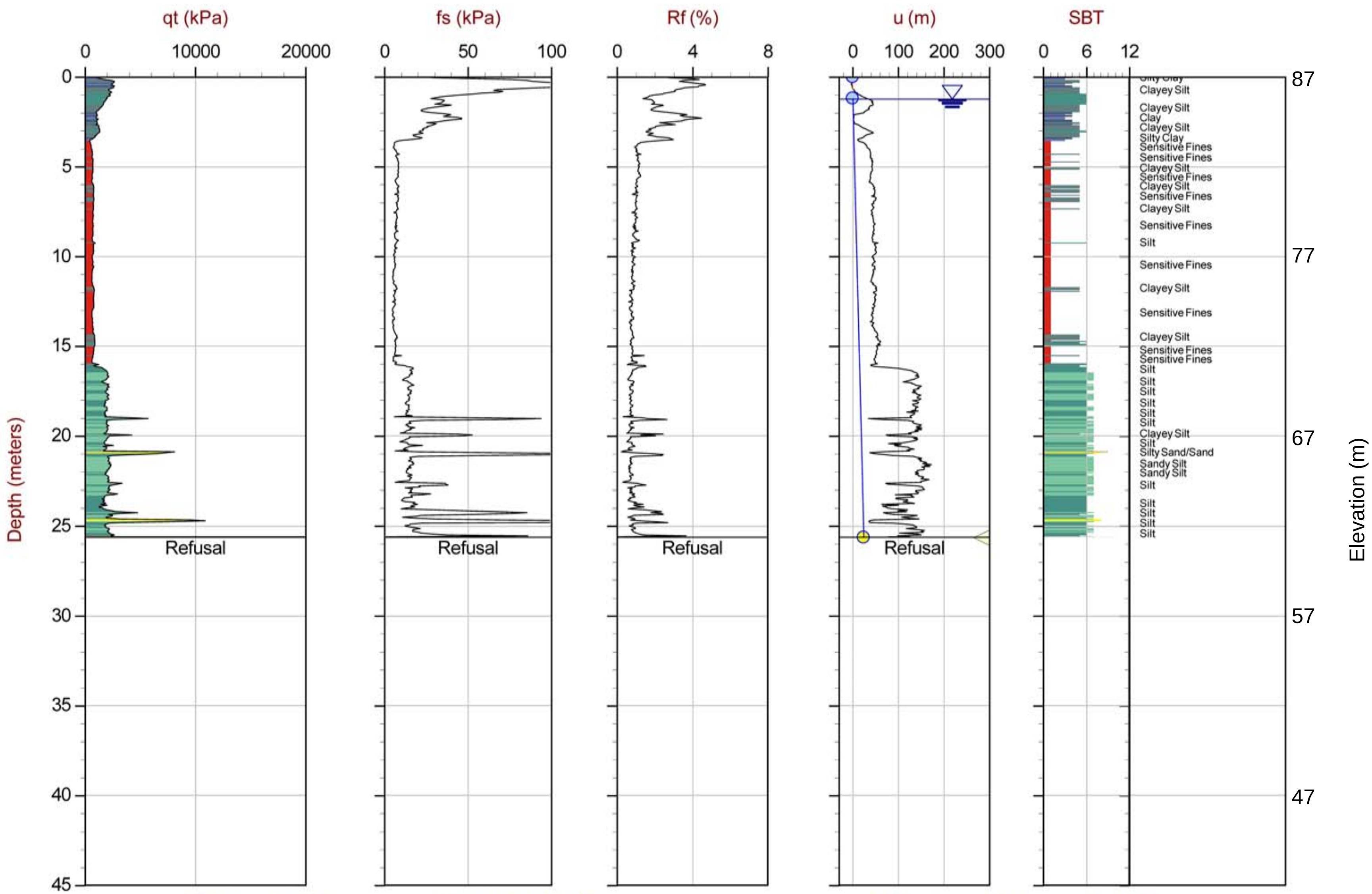

Max Depth: 25.600 m / 83.99 ft
Depth Inc: 0.050 m / 0.164 ft

File: 14-05013_CP03.CR1

SBT: Robertson and Campanella, 1986
Coords: UTM Zone 18 N: 5043741 E: 400907

Fig. B-4. Non-normalized Plots – CPT-03

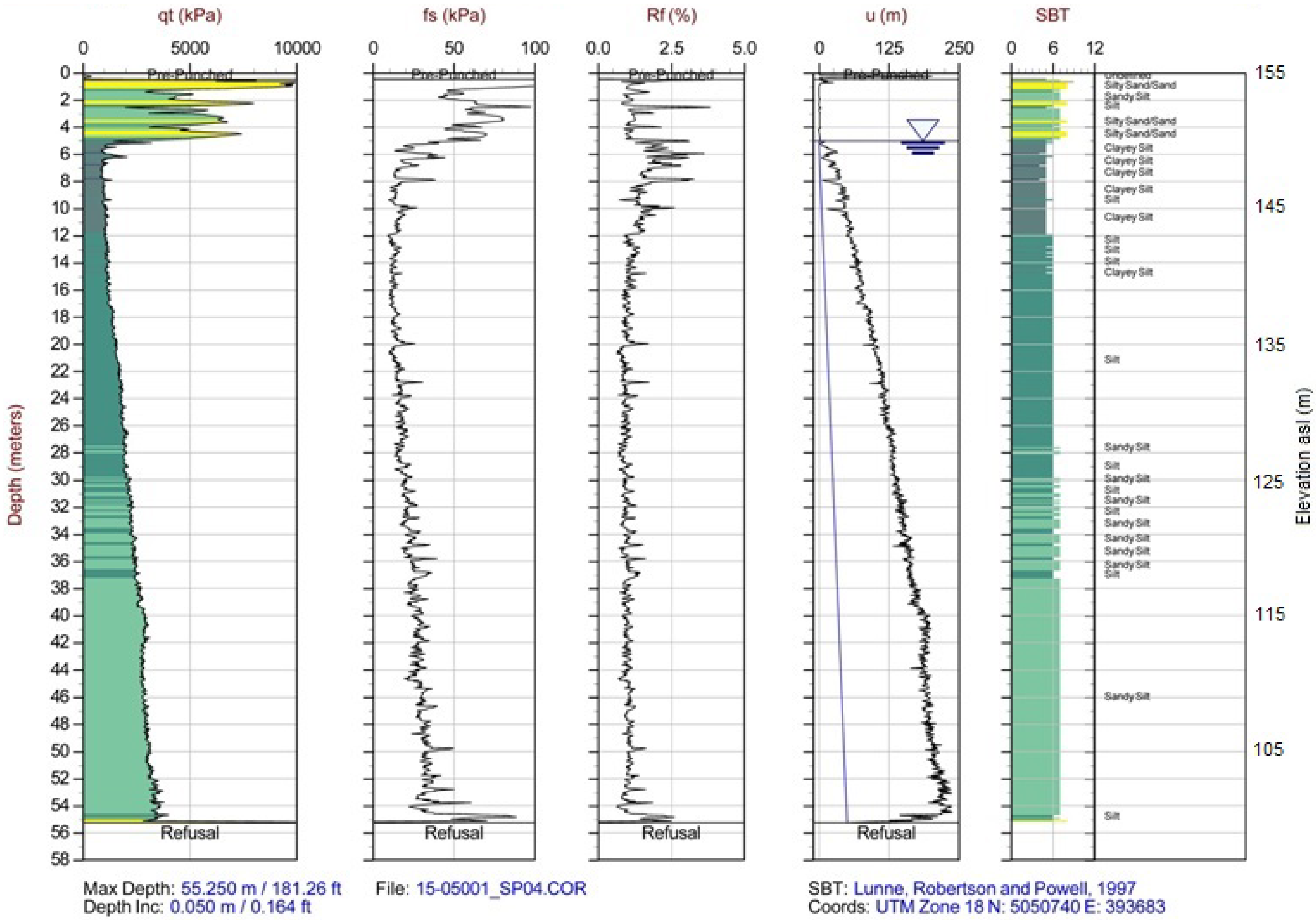

Fig. B-5. Non-normalized Plots – CPT-04

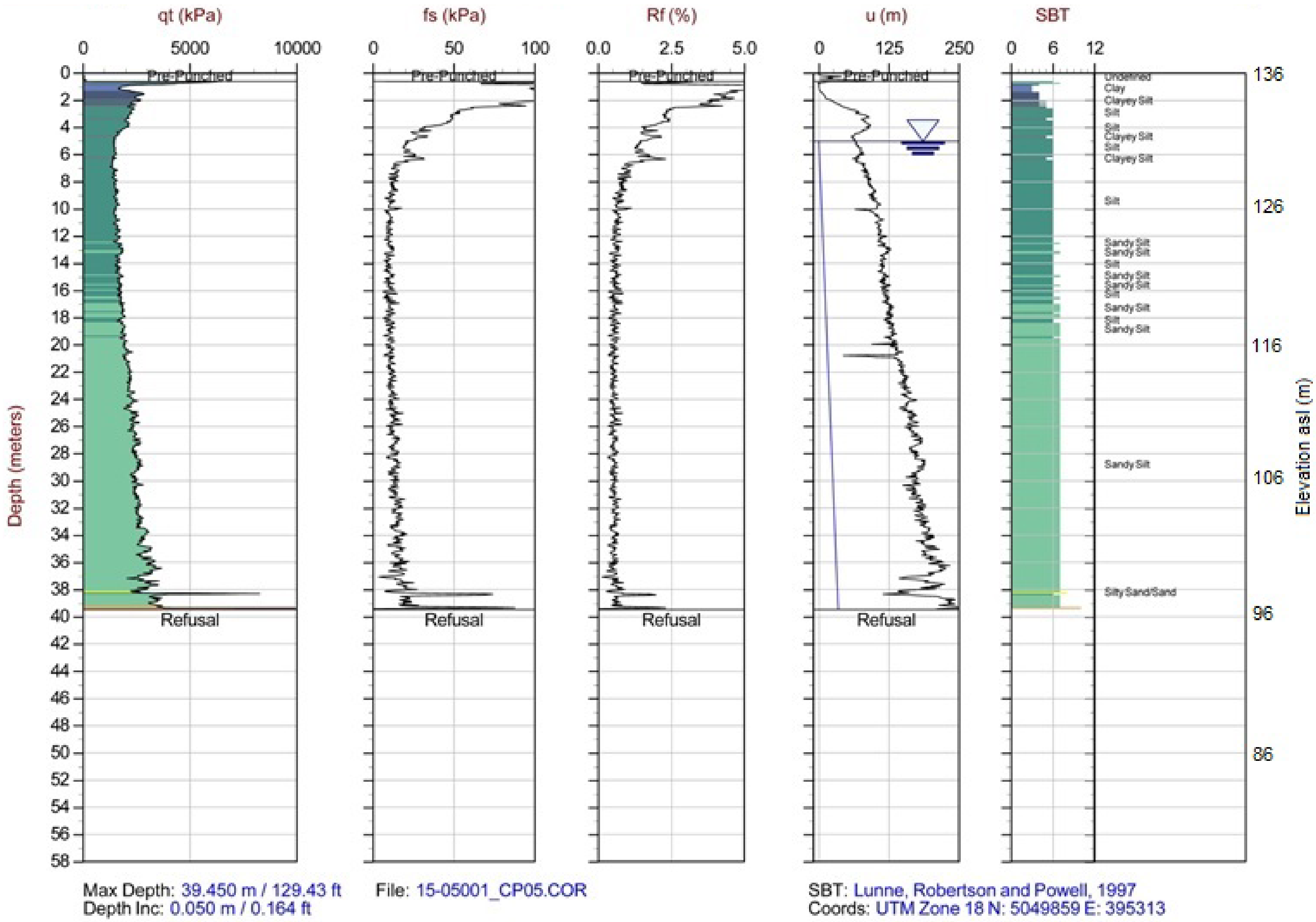

Fig. B-6. Non-normalized Plots – CPT-05

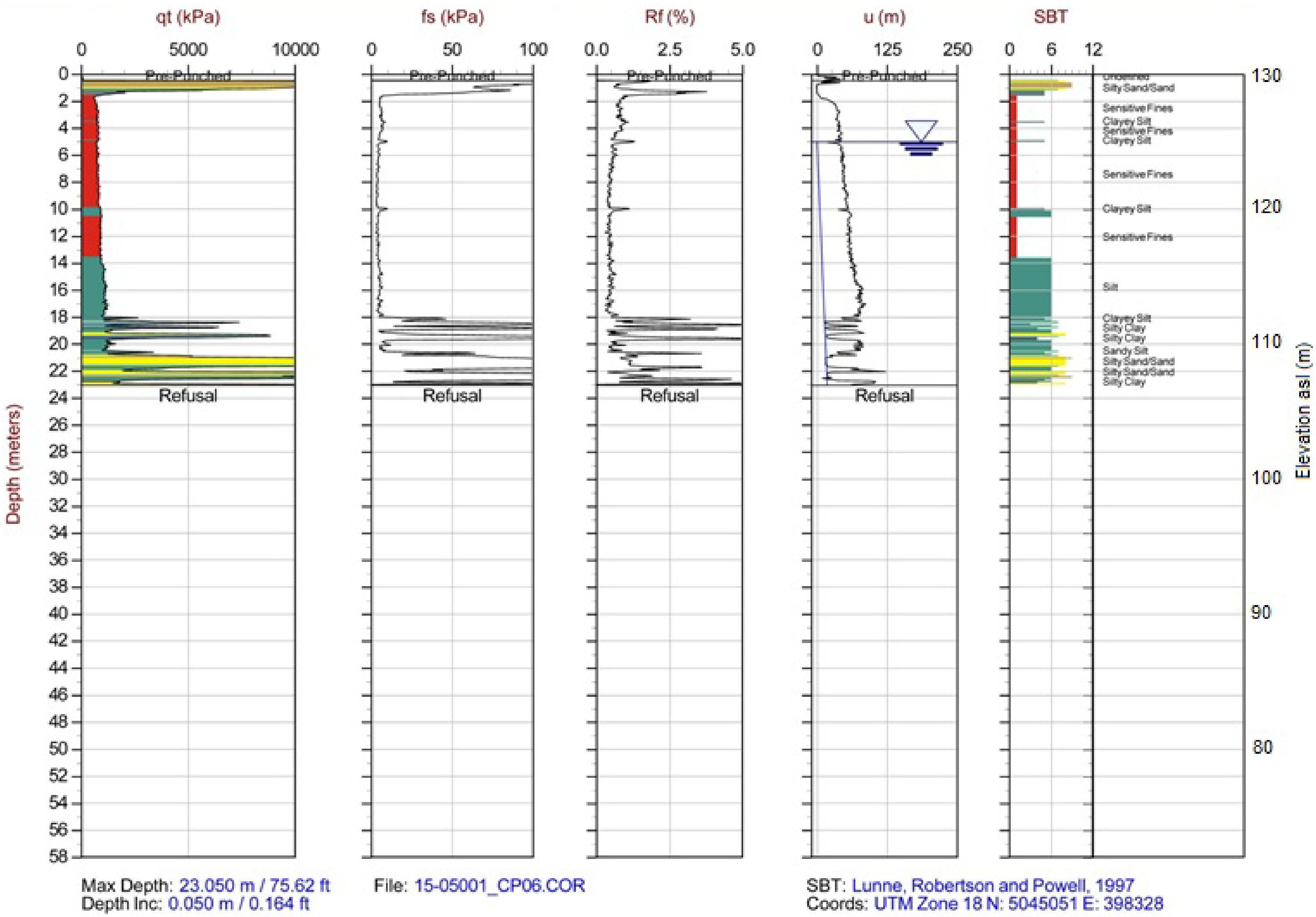

Fig. B-7. Non-normalized Plots – CPT-06

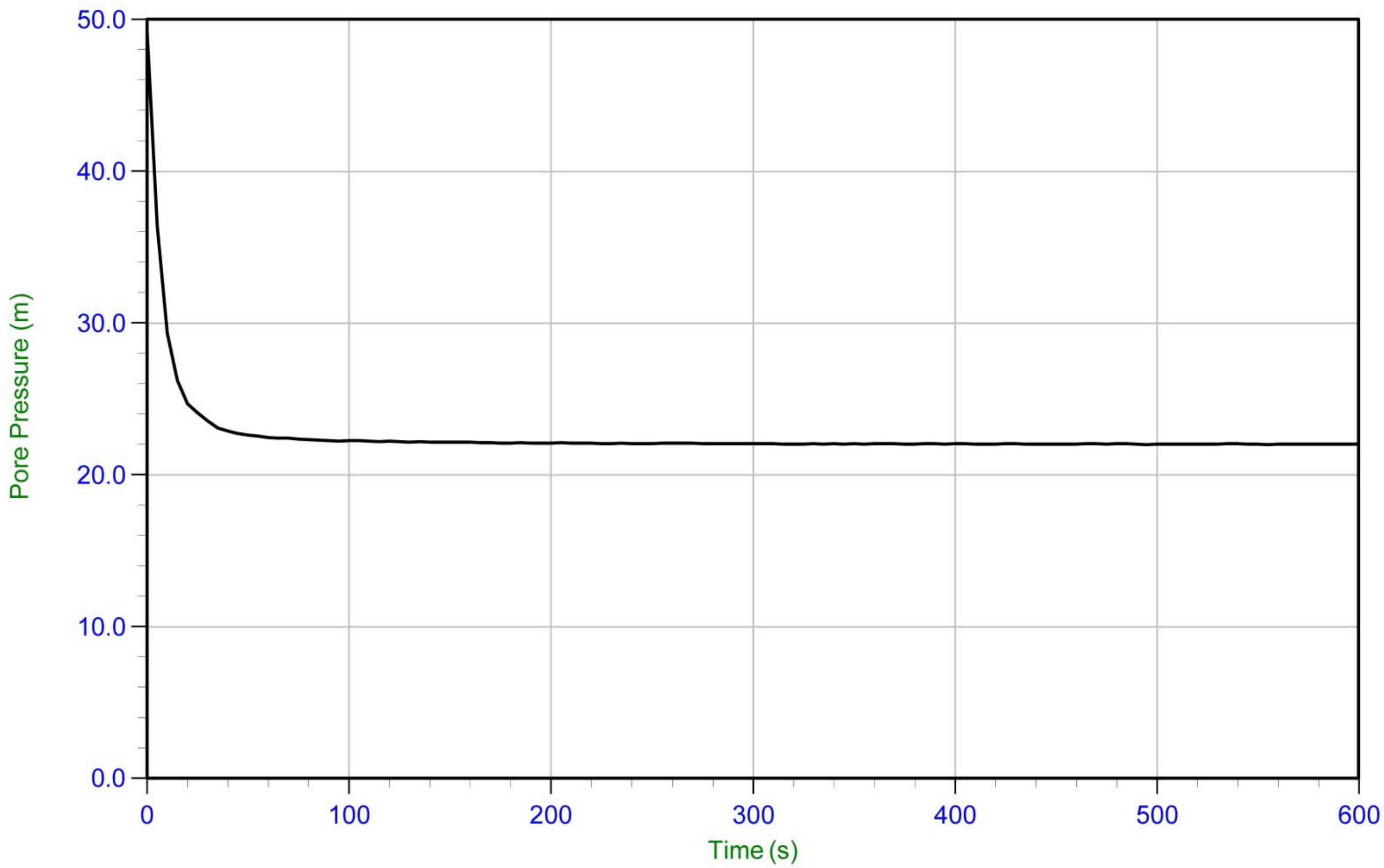

Fig. B-8. Pore Pressure Dissipation Test Plot – CPT-01 (Depth 31.85 m)

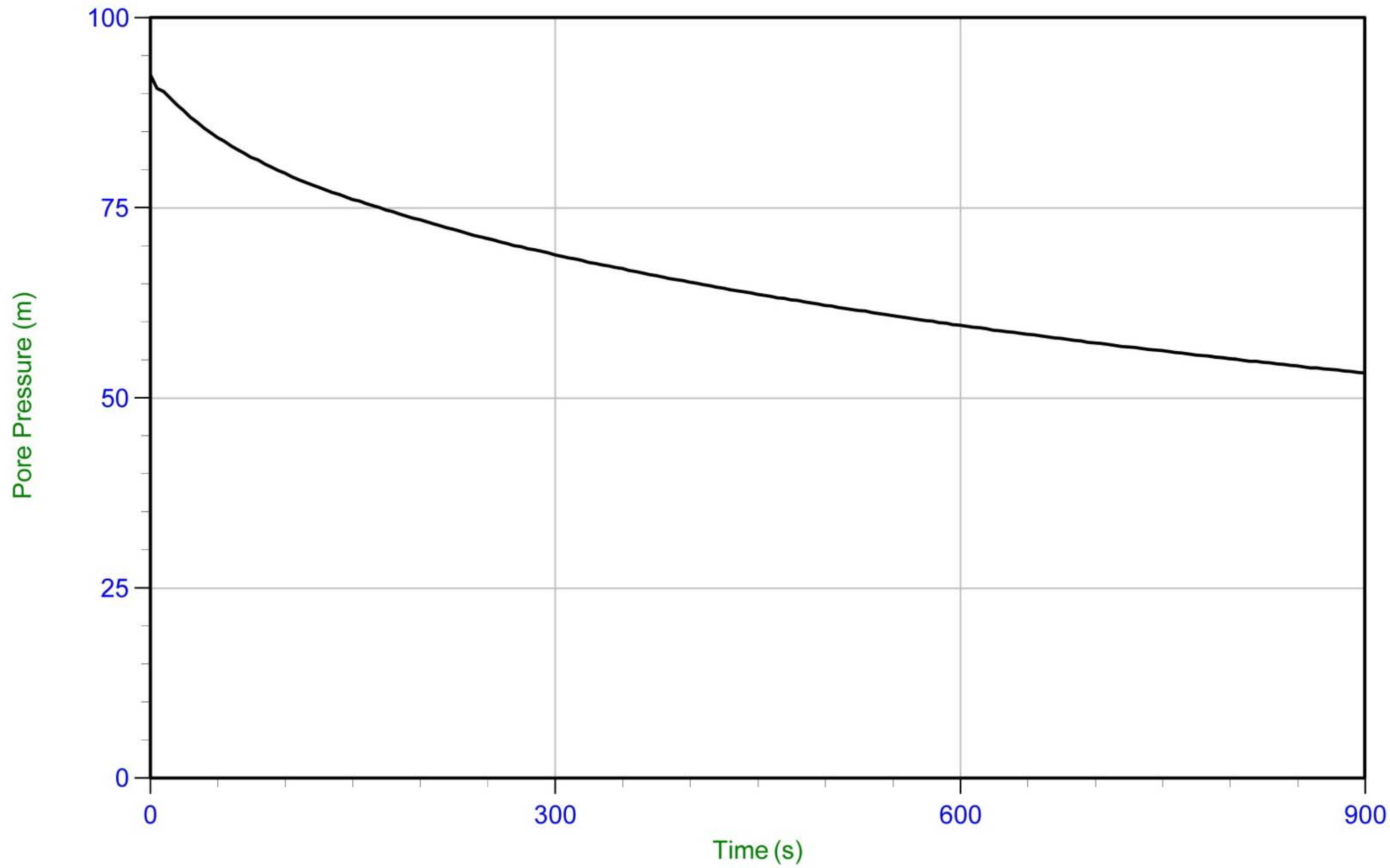

Fig. B-9. Pore Pressure Dissipation Test Plot – CPT-01A (Depth 24.85 m)

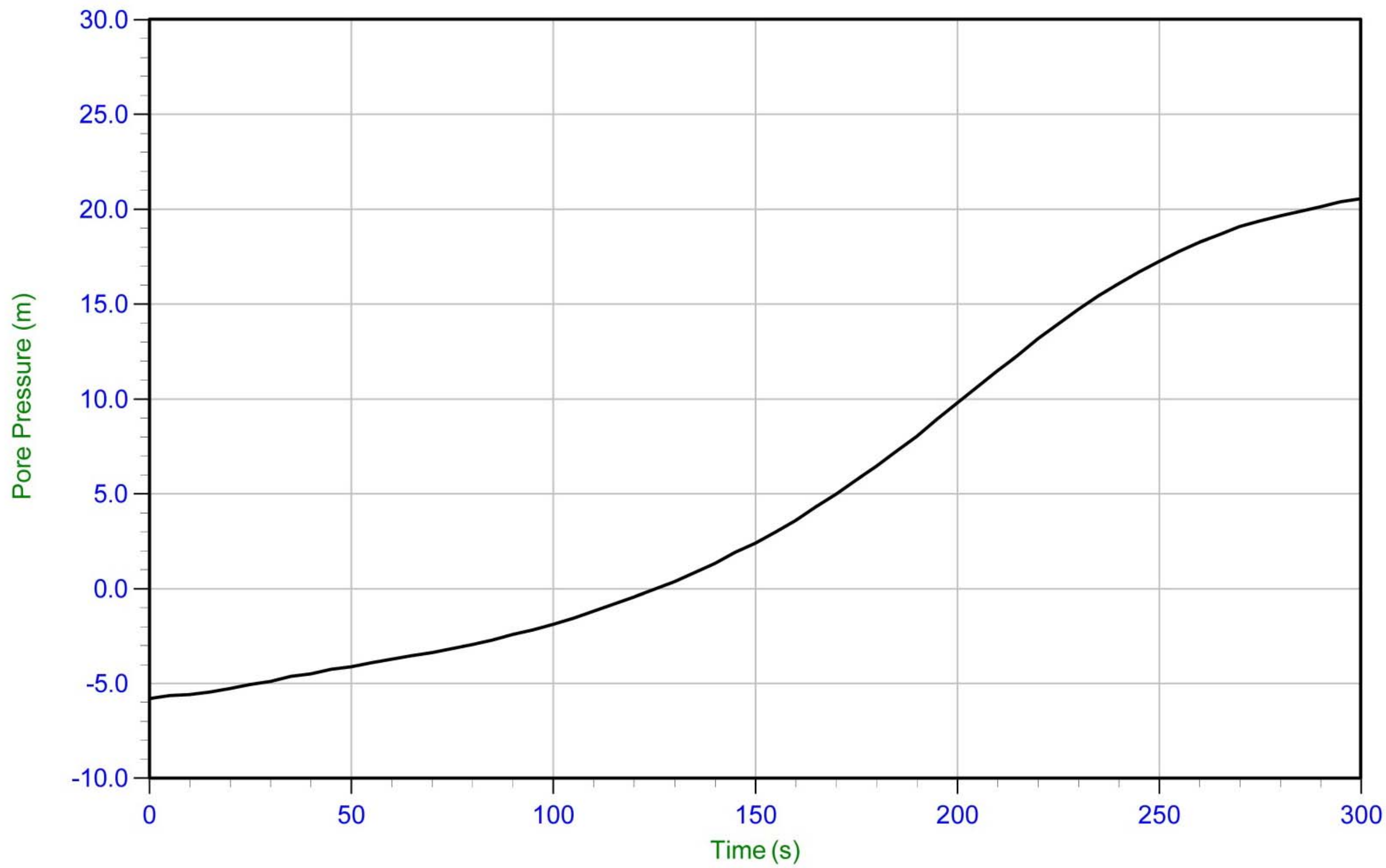

Fig. B-10. Pore Pressure Dissipation Test Plot – CPT-01A (Depth 33.55 m)

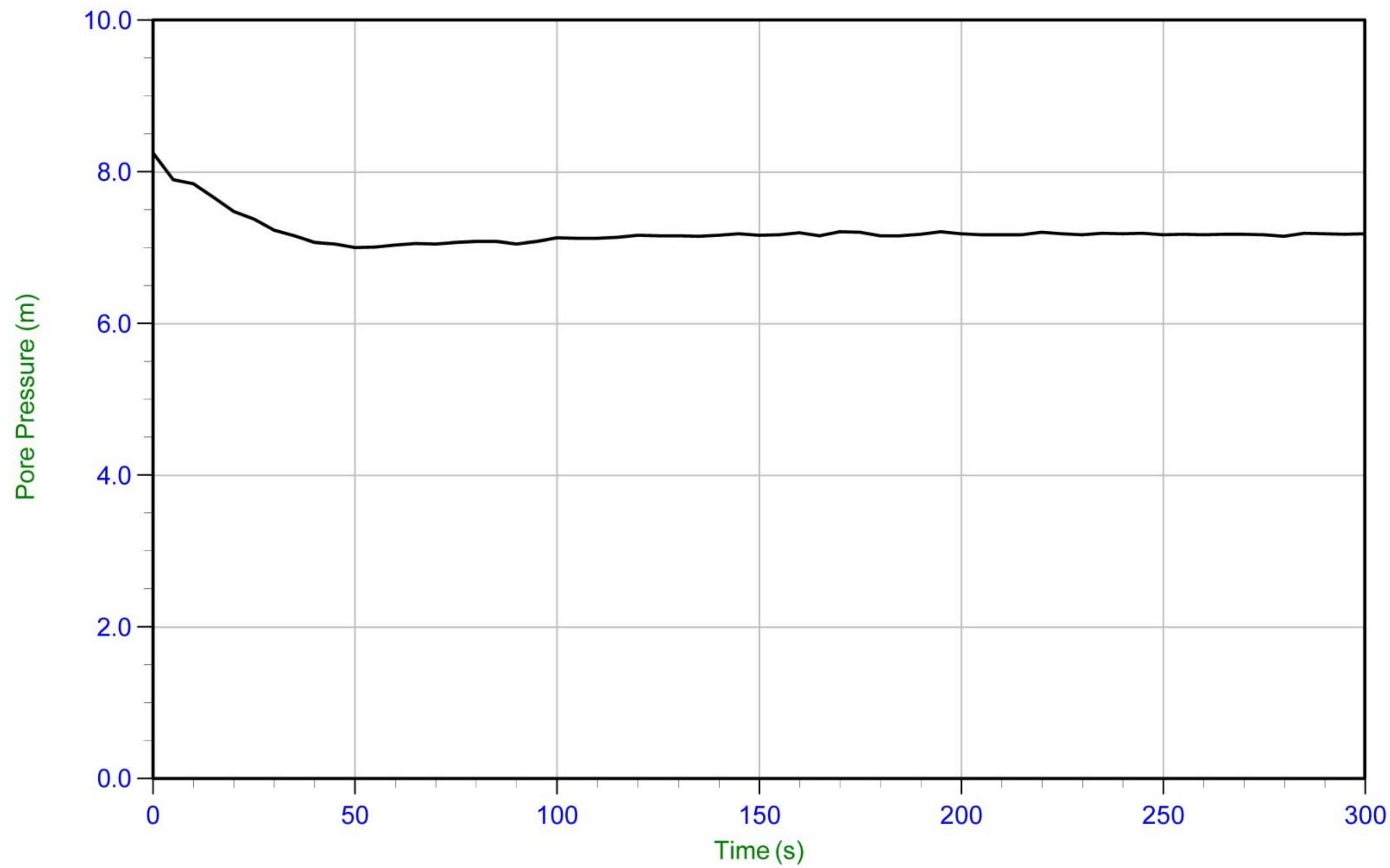

Fig. B-11. Pore Pressure Dissipation Test Plot – CPT-02 (Depth 7.00 m)

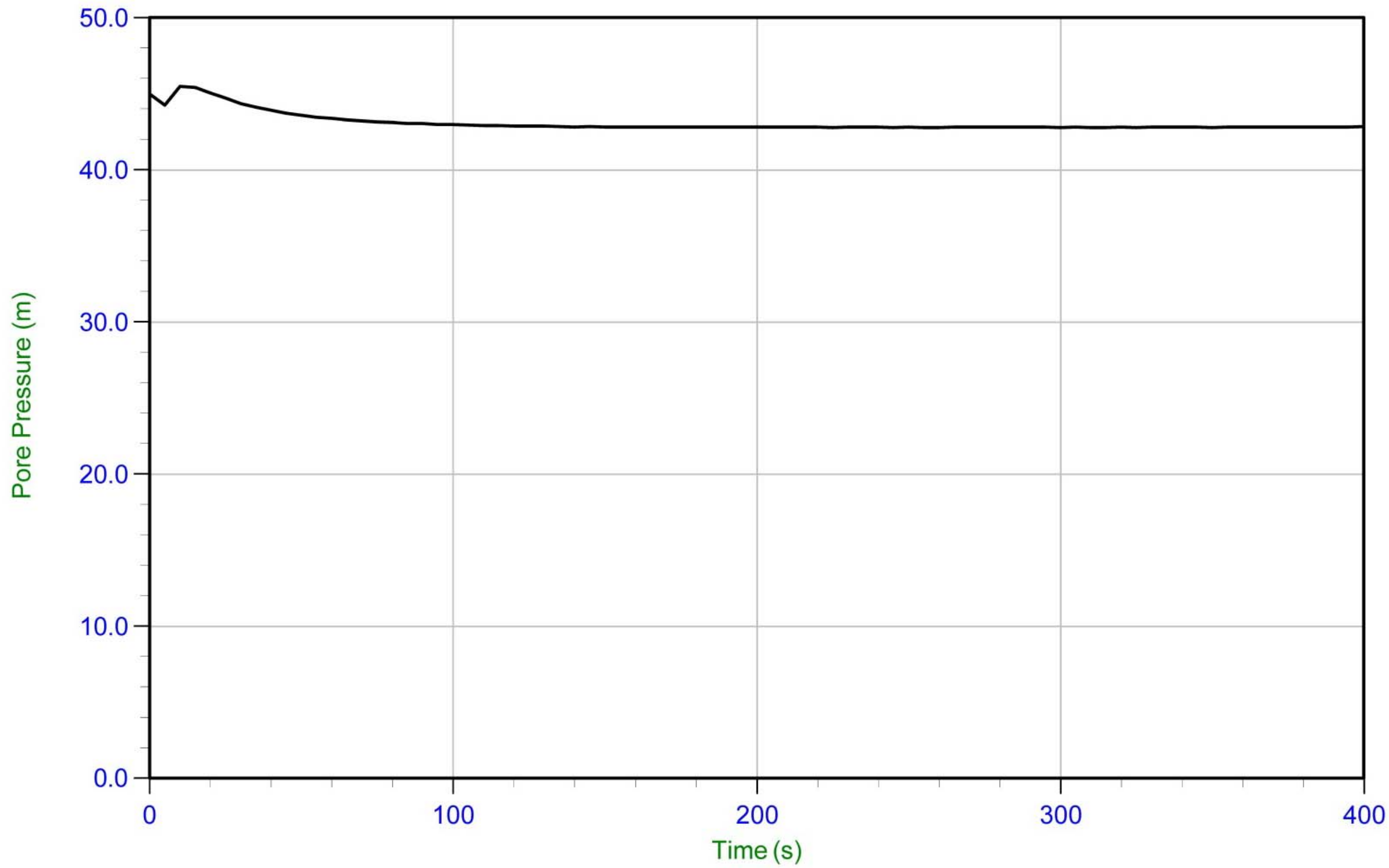

Fig. B-12. Pore Pressure Dissipation Test Plot – CPT-02 (Depth 34.50 m)

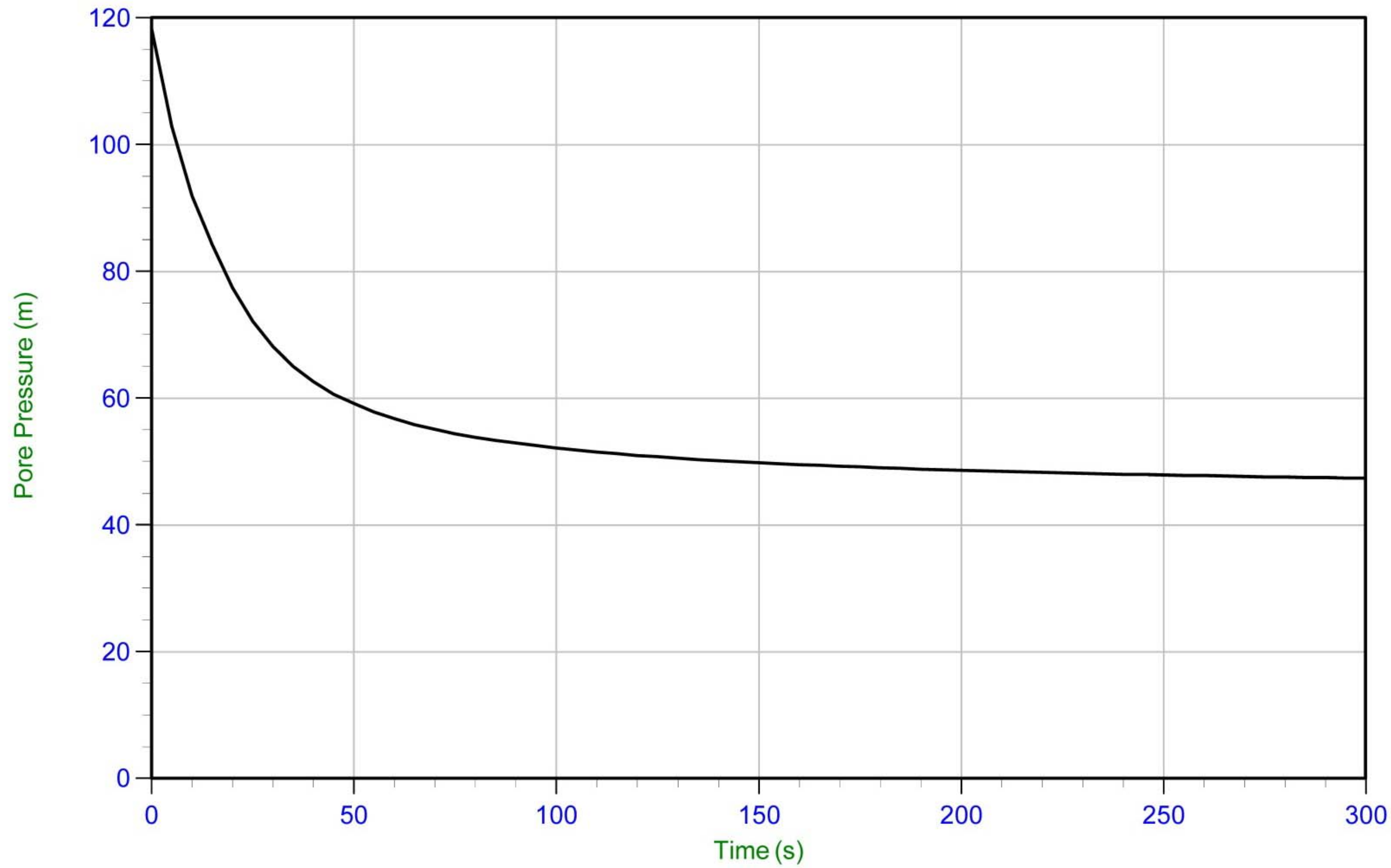

Fig. B-13. Pore Pressure Dissipation Test Plot – CPT-02 (Depth 36.70 m)

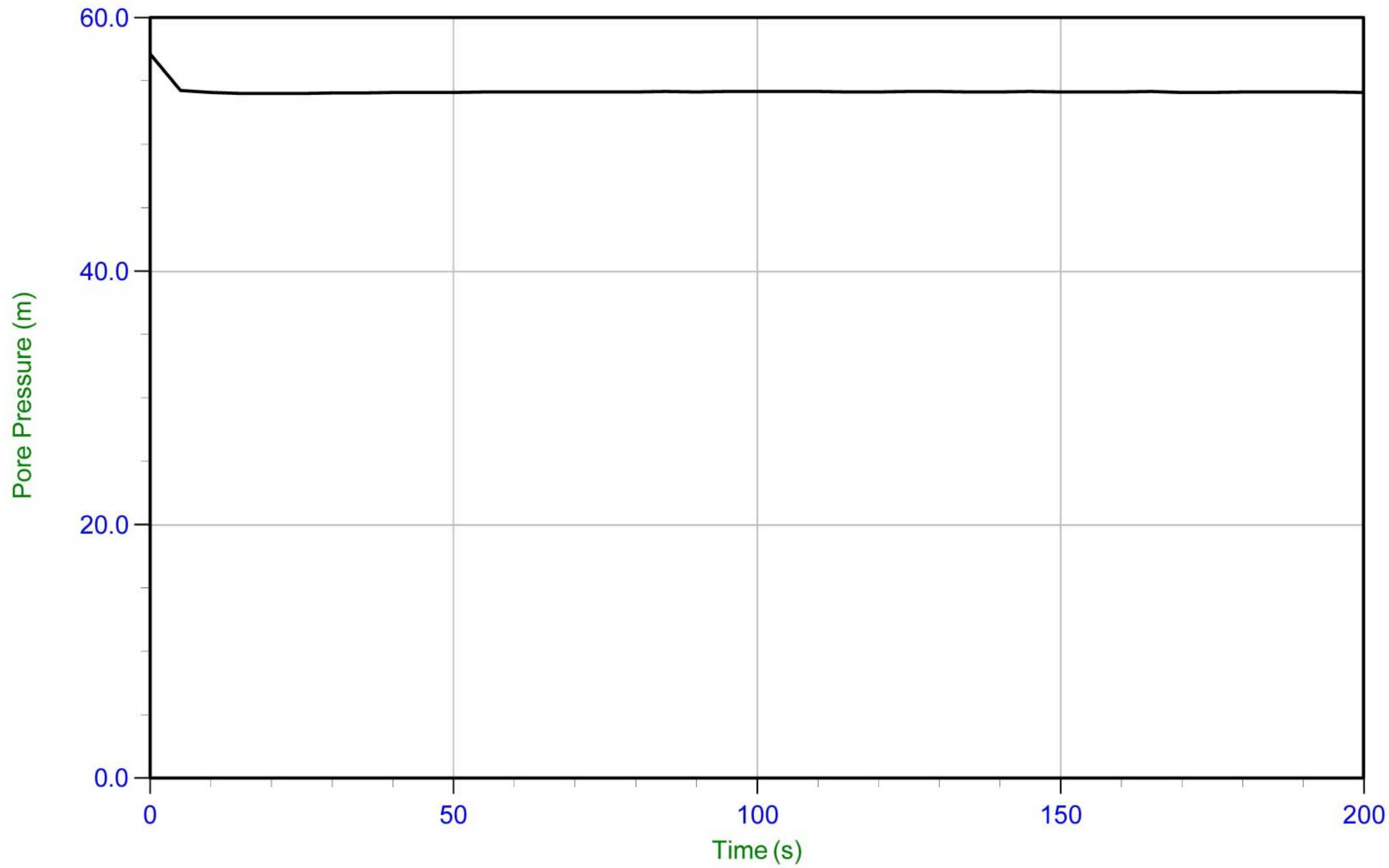

Fig. B-14. Pore Pressure Dissipation Test Plot – CPT-02 (Depth 43.70 m)

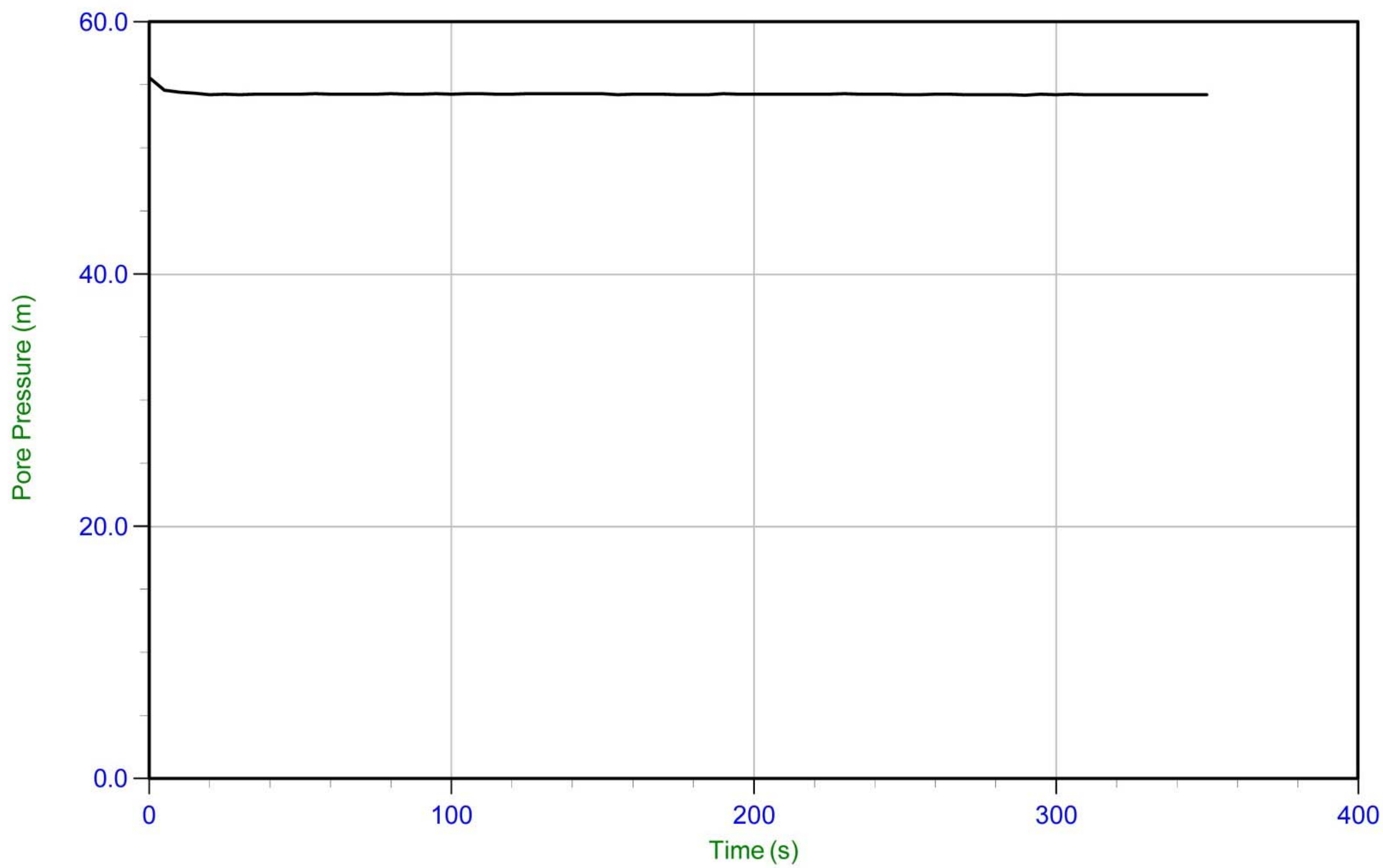

Fig. B-15. Pore Pressure Dissipation Test Plot – CPT-02 (Depth 43.90 m)

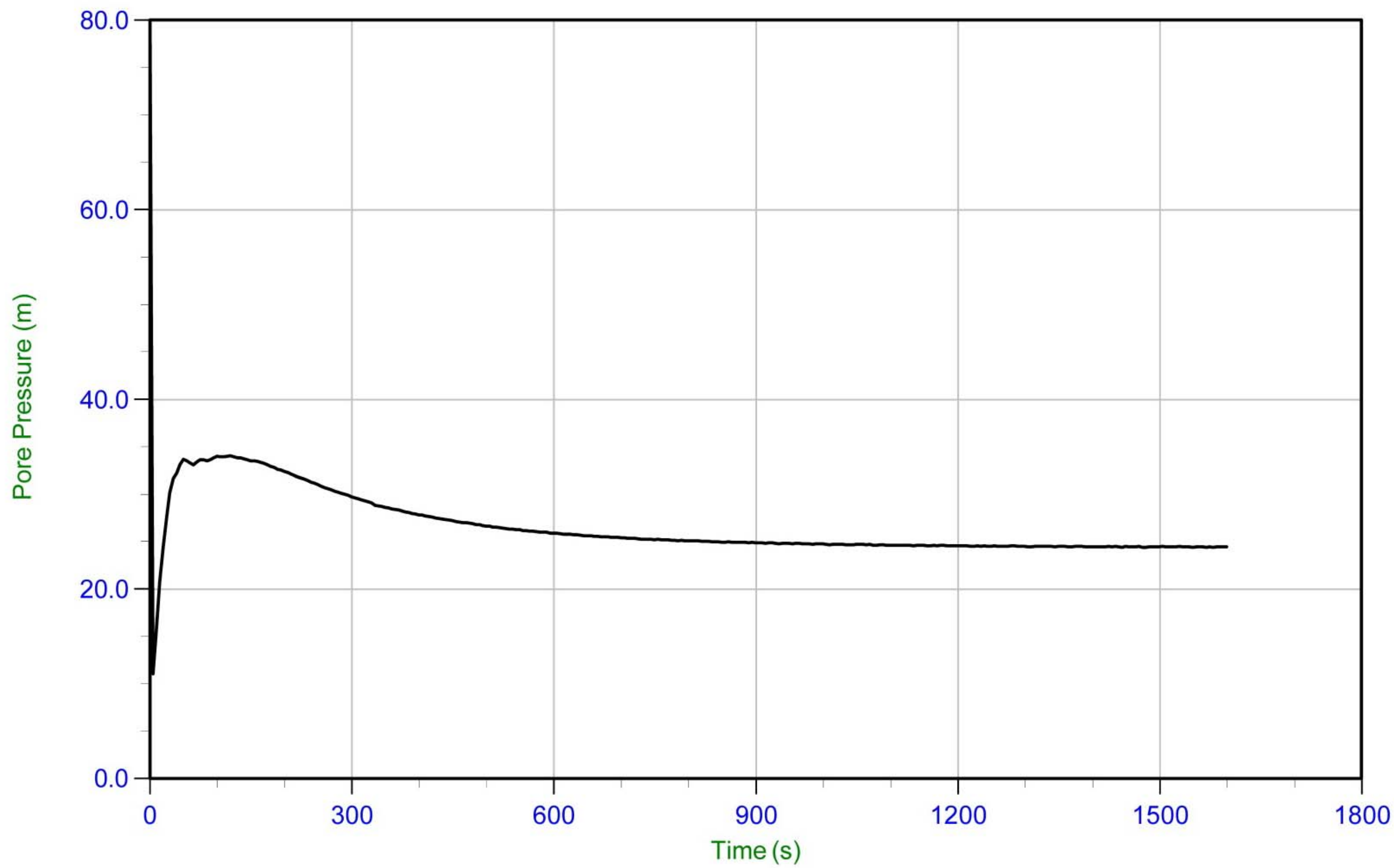

Fig. B-16. Pore Pressure Dissipation Test Plot – CPT-03 (Depth 25.65 m)

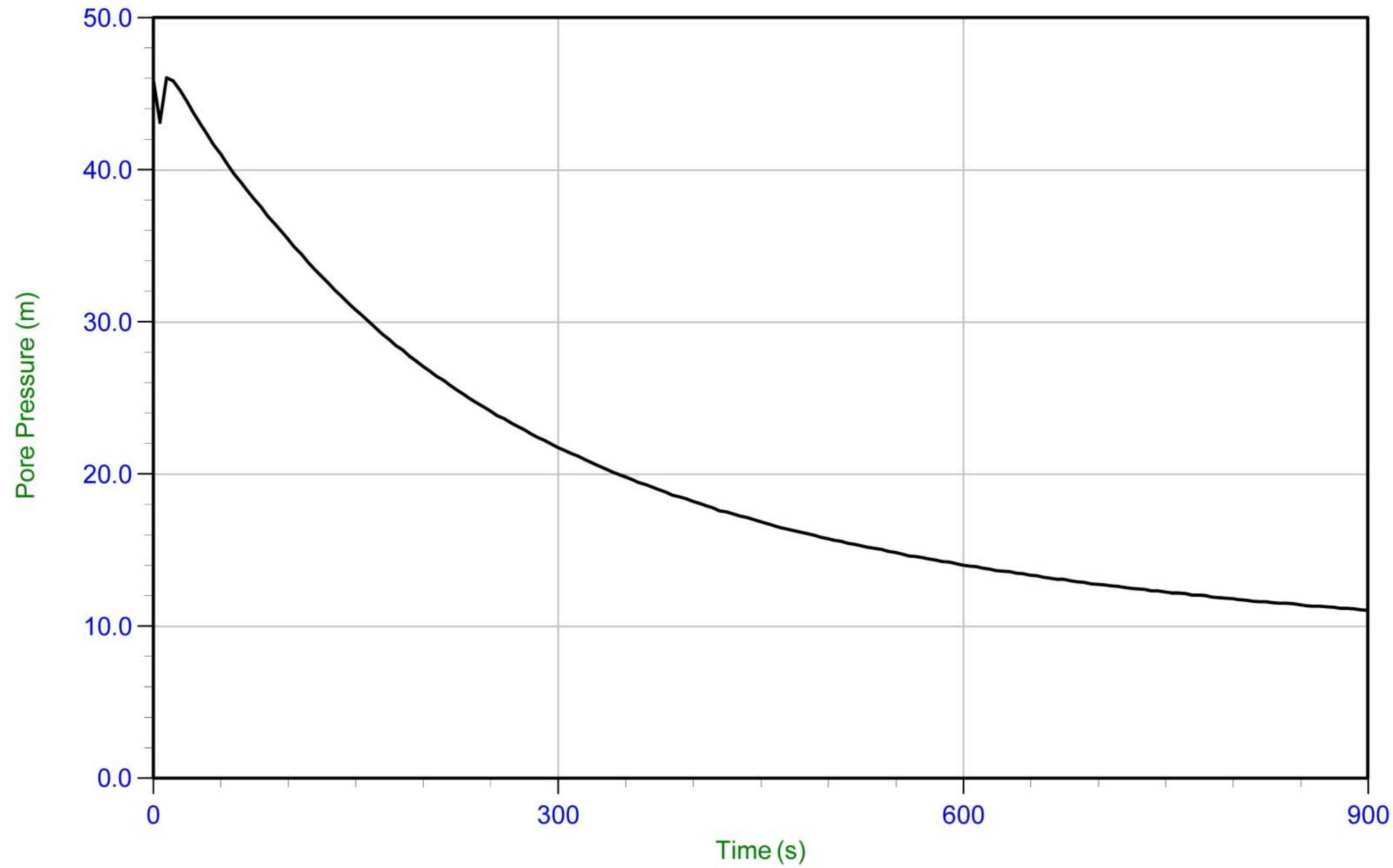

Fig. B-17. Pore Pressure Dissipation Test Plot – CPT-04 (Depth 10.00 m)

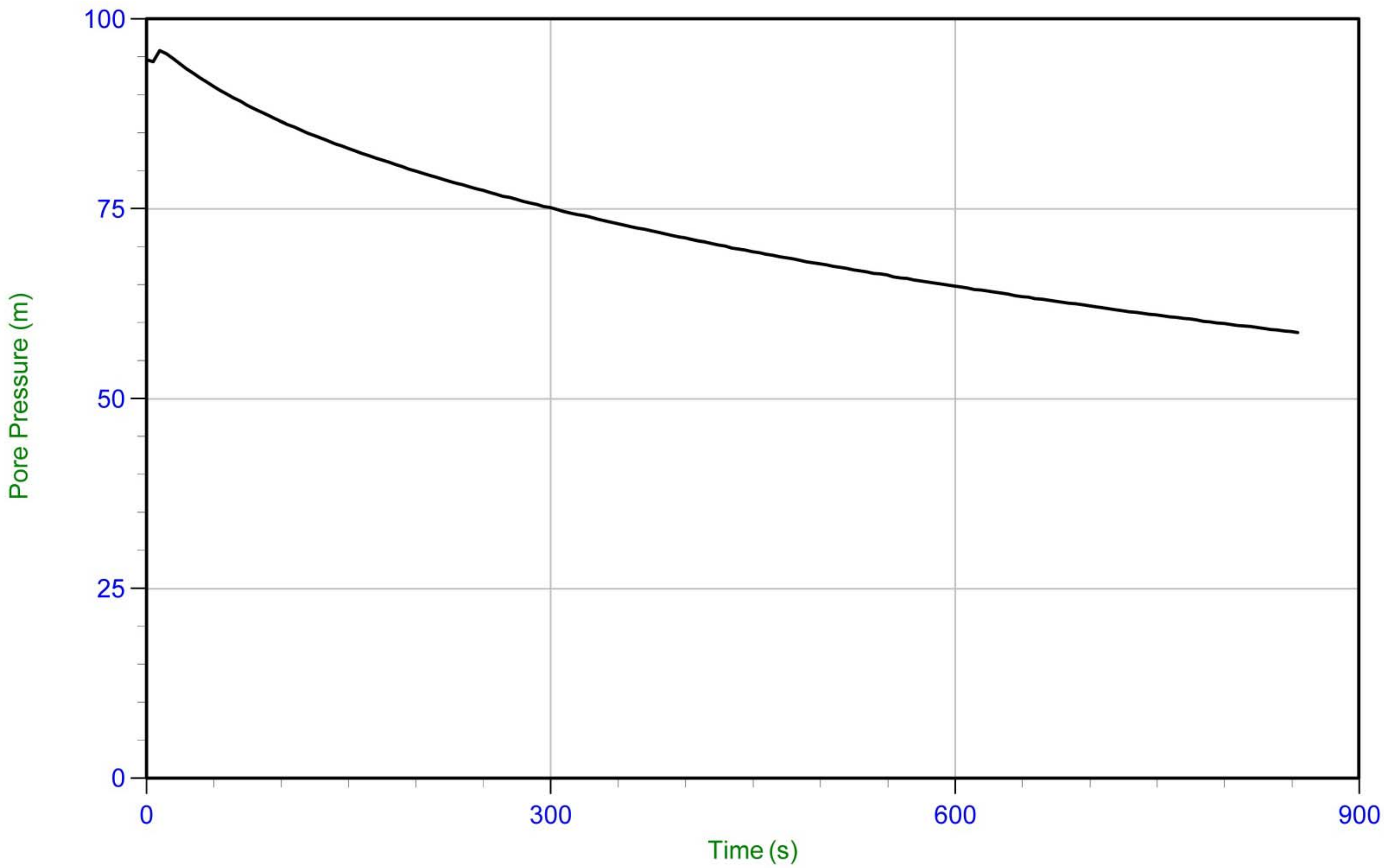

Fig. B-18. Pore Pressure Dissipation Test Plot – CPT-04 (Depth 20.00 m)

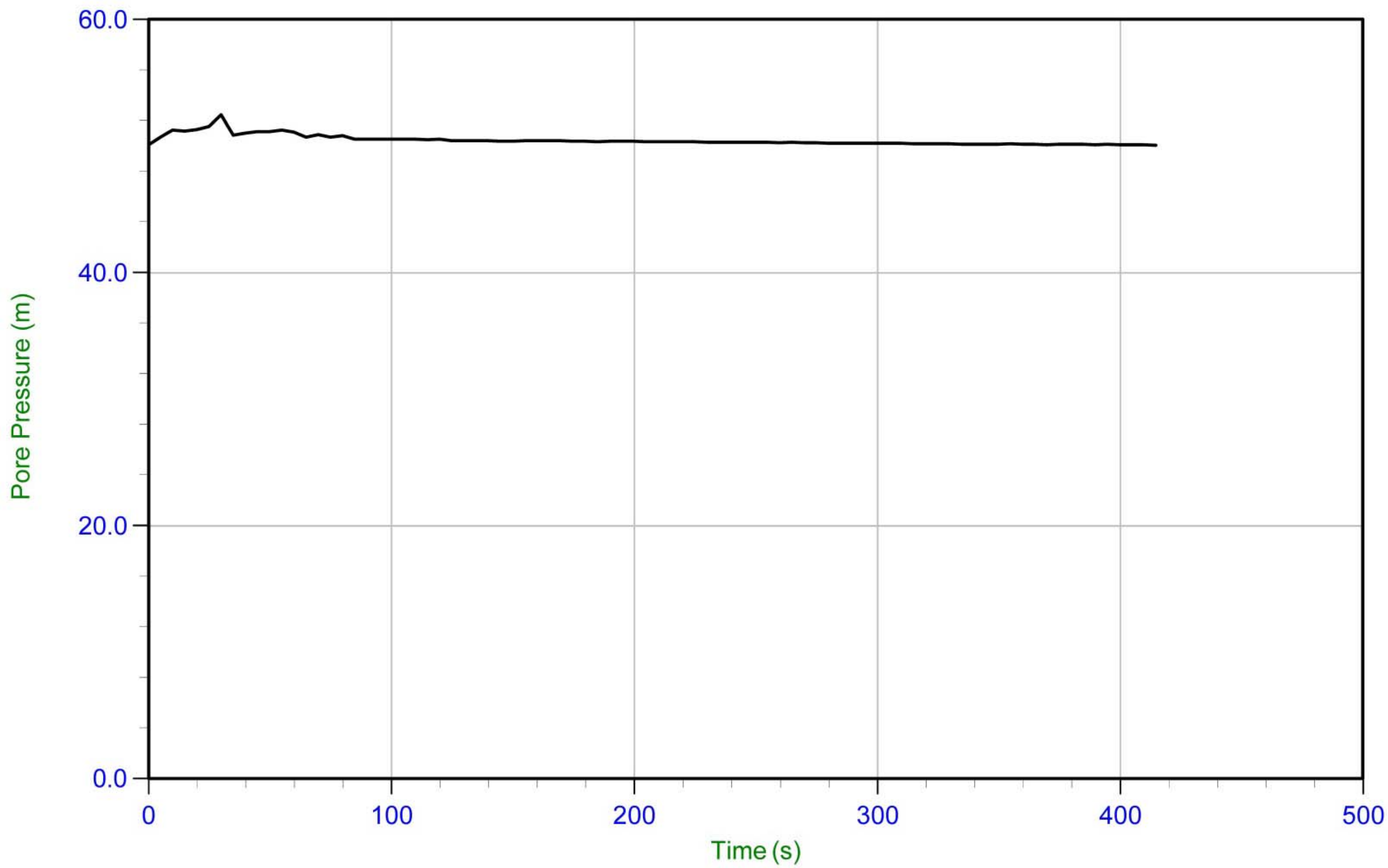

Fig. B-19. Pore Pressure Dissipation Test Plot – CPT-04 (Depth 55.25 m)

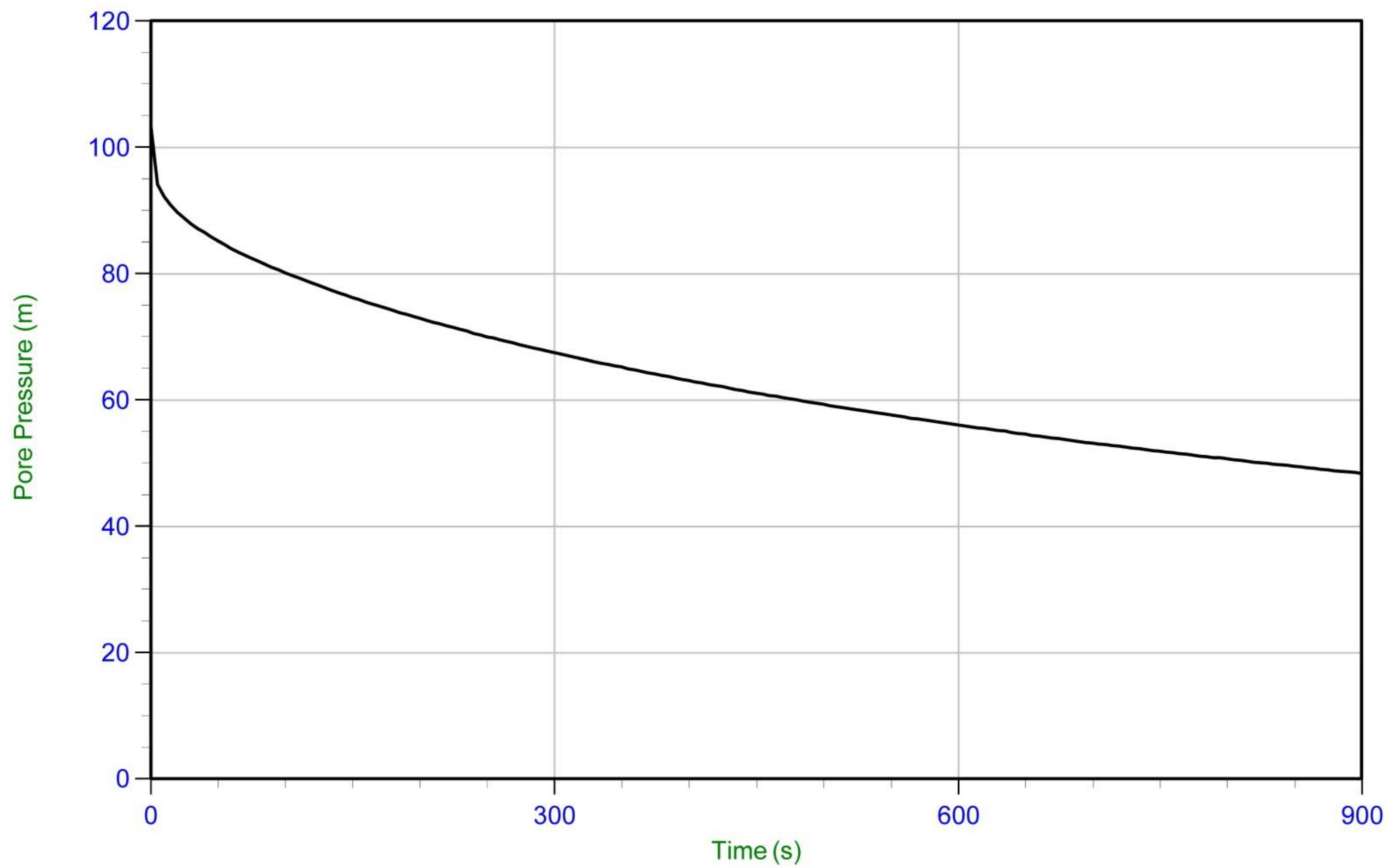

Fig. B-20. Pore Pressure Dissipation Test Plot – CPT-05 (Depth 10.00 m)

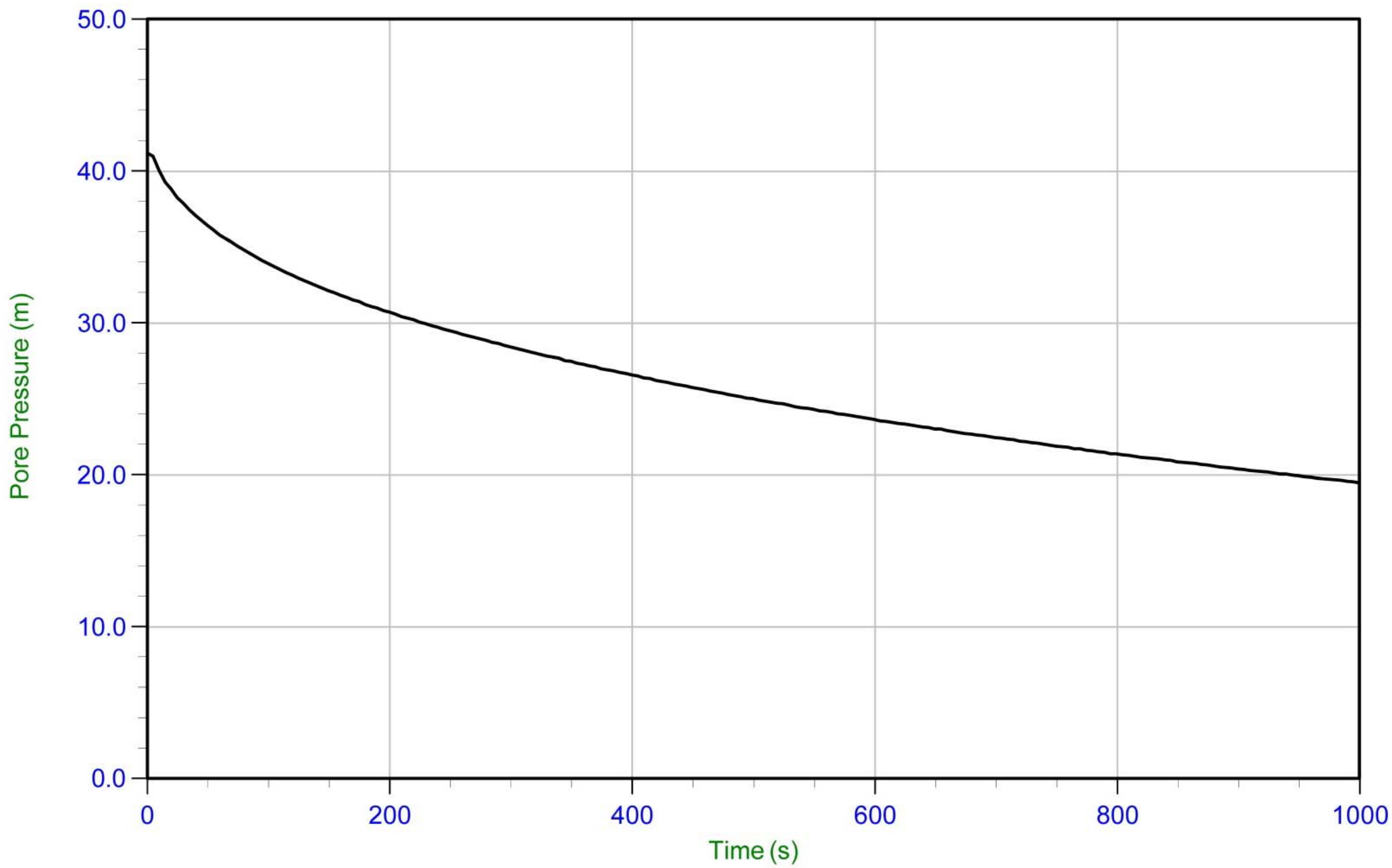

Fig. B-21. Pore Pressure Dissipation Test Plot – CPT-06 (Depth 5.00 m)

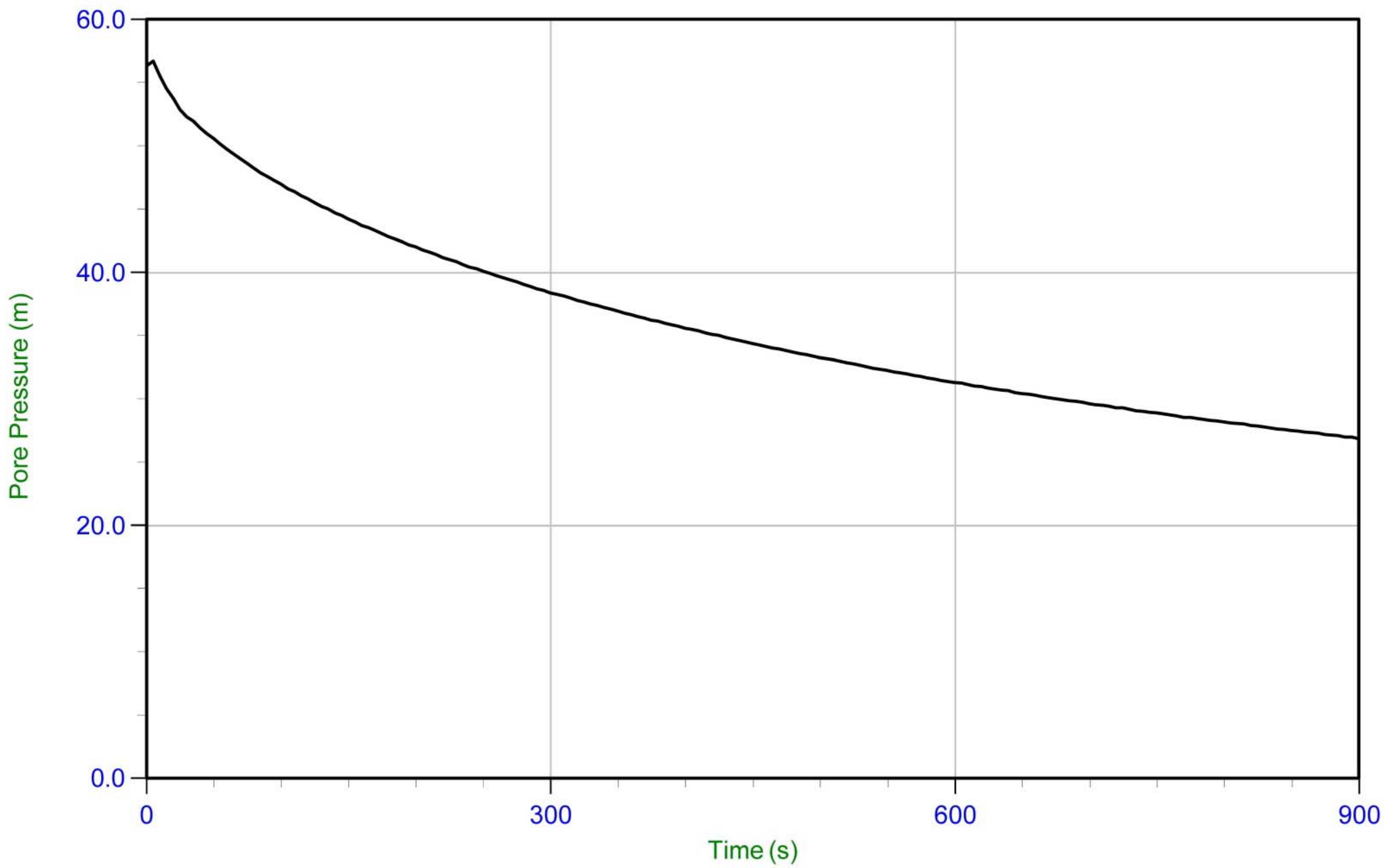

Fig. B-22. Pore Pressure Dissipation Test Plot – CPT-06 (Depth 10.00 m)

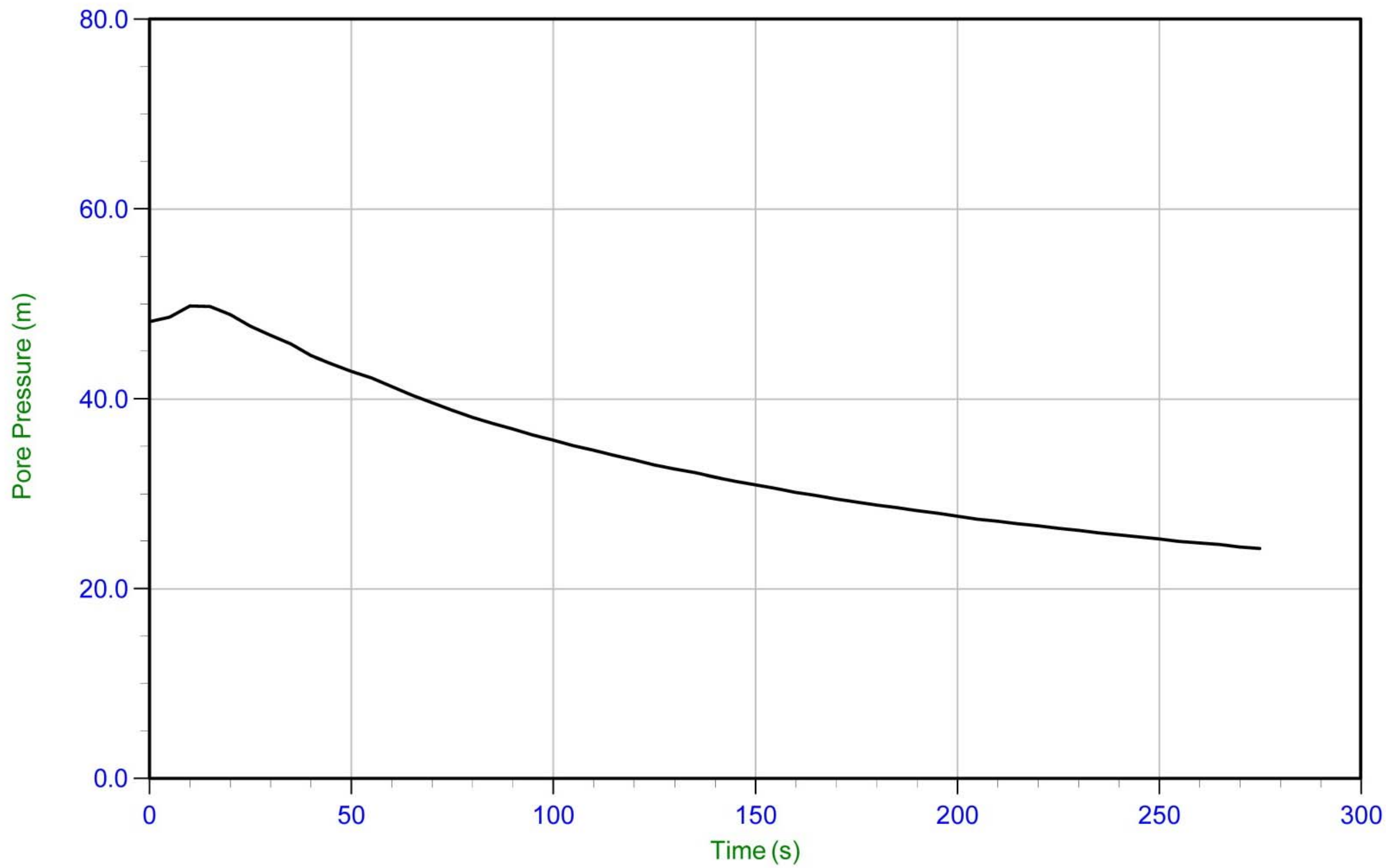

Fig. B-23. Pore Pressure Dissipation Test Plot – CPT-06 (Depth 23.05 m)